Journal of Environmental Chemical Engineering 12 (2024) 114457

Contents lists available at ScienceDirect

Journal of Environmental Chemical Engineering

journal homepage: www.elsevier.com/locate/jece

Recovery and fractionation of volatile fatty acids from fermented solutions by electrodialysis: electrochemical characterization of anion-exchange membranes

Kayo Santana Barros [a,b,*], Bruno C. Marreiros [c,d], Maria A.M. Reis [c,d], João Goulão Crespo [b,e], Valentín Pérez-Herranz [a], Svetlozar Velizarov [b]

[a] IEC Group, ISIRYM, Universitat Politècnica de València, Camí de Vera s/n, 46022, P.O. Box 22012, València E-46071, Spain
[b] LAQV / REQUIMTE, Department of Chemistry, NOVA School of Science and Technology, NOVA FCT, Universidade NOVA de Lisboa, Caparica 2829-516, Portugal
[c] Associate Laboratory i4HB - Institute for Health and Bioeconomy, NOVA School of Science and Technology, Universidade NOVA de Lisboa, Caparica 2829-516, Portugal
[d] UCIBIO – Applied Molecular Biosciences Unit, Department of Chemistry, NOVA School of Science and Technology, Universidade NOVA de Lisboa, Caparica 2829-516, Portugal
[e] ITQB, Universidade NOVA de Lisboa, Av. da República, Oeiras 2780-157, Portugal

ARTICLE INFO

Keywords:
PHA precursors
Fractionation of VFAs, membrane-based process
Linear sweep voltammetry, chronopotentiometry

ABSTRACT

Electrodialysis can be used to recover charged precursors, such as volatile fatty acids (VFAs), of the biopolymers polyhydroxyalkanoates (PHAs). In general, all VFAs are recovered in a receiver solution, despite their advantageous partial fractionation. Herein, the separation of acetic, propionic, butyric, and valeric acids by electrodialysis was evaluated using three anion-exchange membranes (namely, Ralex AMH-PES, Fumasep FAS-PET-130 and PC200D) applying cell voltages from 0 V to 2.88 V. The mass transfer mechanisms were evaluated by linear sweep voltammetry and chronopotentiometry. Fumasep showed a slightly greater VFAs fractionation capacity than Ralex, while it was much greater for PC200D due to the presence of tertiary amines in its fixed functional groups. Overall, increasing the operating voltage and/or time reduced the degree of VFAs fractionation with all membranes. The higher percent extraction values and greater VFAs fractionation degrees obtained with the PC200D membrane could enhance PHAs storage efficiency.

1. Introduction

Polyhydroxyalkanoates (PHA) are polymers synthesized by microorganisms, serving as intracellular reserves for both carbon and energy. These biopolymers are biodegradable, biocompatible, and display a diverse range of physicochemical characteristics. PHA are considered a sustainable alternative to traditional fossil fuel-based plastics, as their properties and versatility allows for their use in various sectors, including various applications such as agriculture, biomedical, fabrics and coatings [1].

PHAs are classified into three groups based on the length of their monomer side chains, which significantly influence their properties: short-chain-length (scl-PHAs) containing 3–5 carbon units, medium-chain-length (mcl-PHAs) with 6–14 carbon units, and long-chain-length (lcl-PHAs) comprising more than 14 carbon units [1]. Among these categories, scl-PHA stands out as the most common type. Scl-PHA can be composed either of 3-hydroxybutyrate (3HB) monomers forming the homopolymer P3HB or a copolymer P(3HB-co-3HV) consisting of both 3HB and 3-hydroxyvalerate (3HV) monomers, with varying 3HV content.

Molecules such as volatile fatty acids (VFAs) serve as precursors in PHA synthesis, wherein the carbon chain length and composition of VFAs utilized during PHA production play a significant role in determining the resulting properties of PHA. In the production of PHA by mixed microbial cultures (MMCs), acetic, propionic, butyric, and valeric acids frequently serve as PHA precursors, leading to the synthesis of scl-PHA. Specifically, during PHA synthesis, 3HV monomers can derive either from a single molecule of valeric acid or from a combination of acetic and propionic acids in a 1:1 ratio. Similarly, 3HB monomer can be produced either from a single molecule of butyric acid or from a

* Corresponding author at: IEC Group, ISIRYM, Universitat Politècnica de València, Camí de Vera s/n, 46022, P.O. Box 22012, València E-46071, Spain,
E-mail address: kasanbar@alumni.upv.es (K.S. Barros).

https://doi.org/10.1016/j.jece.2024.114457
Received 23 May 2024; Received in revised form 10 September 2024; Accepted 13 October 2024
Available online 15 October 2024

combination of two molecules of acetic acid. Furthermore, each mole of VFA requires 2 moles of ATP for PHA synthesis (1 mol of ATP for active transport and 1 mol of ATP for intracellular conversion). Consequently, VFAs with longer carbon chains, such as butyric and valeric acids, require less ATP to produce 1 Cmol of PHA compared to shorter-chain VFAs (e.g., acetic and propionic acids) [1].

Sustainable development trends, driven by governmental regulations and incentives, are boosting the PHA industry. Globally, the PHA industry market value is projected to increase from €85 million in 2023 to €178 million in 2028, at a compound annual growth rate (CAGR) of 15.9 % [2]. Nonetheless, despite over a decade of investigation, prices for PHAs remain higher compared to conventional plastics, particularly for lower-grade applications such as packaging [1]. Therefore, it is imperative to develop and optimize the PHA production process, focusing on reducing resource usage, production costs, and expanding the structural diversity of PHA. Addressing these challenges could involve recovering and fractionating VFAs, the key precursors for PHA, from fermented solutions typically used in PHA production with MMCs. Specifically, producing PHA from solutions enriched with butyric and valeric acids, recovered from fermented streams (comprising acetic, propionic, butyric, and valeric acids) obtained via acidogenic fermentation of complex organic resources, could significantly enhance control and efficiency during PHA accumulation. The use of butyric and valeric acids, rather than smaller-chain VFAs like acetic and propionic acids, contributes to higher PHA yields. Moreover, improved control over the VFA mixture composition enables the tailoring of PHA monomeric structure (e.g., producing P(3HB-co-3HV) with 30 % 3HV content, which is more suitable for packaging applications), thus unlocking the potential for novel or enhanced applications that would be difficult to achieve with fermented solutions containing all four VFAs as constituents.

The separation and fractionation of VFAs can be achieved by means of membrane-based processes, such as nanofiltration, Donnan dialysis, conventional electrodialysis and electrodialysis with bipolar membranes [3,4]. Among these techniques, electrodialysis is the most frequently considered, because it allows for the VFAs recovery, in an efficient and eco-friendly manner, which does not require the addition of reagents to the feed solution [4].

Electrodialysis (ED) is an electro-membrane separation process that allows for ion separation by means of the application of an electric potential difference to a cell containing alternating anion- (AEM) and cation-exchange membranes (CEM) [5]. ED has been so far tested in studies aiming the extraction of VFAs from fermented solutions, where VFAs migrate through an AEM towards a receiver (concentrate) solution generally composed of inorganic salts, while nutrients are retained in the feed (diluate) solution. These works have been generally conducted using one type of commercial AEM, applying a constant voltage or current density, aiming at recovering all present VFAs in the receiver solution [6,7].

It has been found that the transport of VFAs through AEMs is accomplished with a slight fractionation between them due to their similar pKa values (~ 4.8), similar molecular dimensions and ion mobilities in the membrane phase [6,8]. However, the works published so far in the literature are not dedicated to evaluating the performance of distinct AEMs, although the membrane properties can affect the degree of VFAs fractionation. The sorption of VFAs in the membranes has also generally not been considered in the studies published so far, despite this phenomenon could block ionic pathways through the polymer, thus reducing the membrane conductivity [9,10]. There is also a lack of studies elucidating the mechanisms that govern the VFAs transport under different current/voltage conditions, which strongly affects the selective ion transfer and energy consumption [11]. To conduct these assessments, various electrochemical techniques can be used, such as impedance spectroscopy, linear sweep voltammetry, cyclic voltammetry and chronopotentiometry. Among these techniques, chronopotentiometry stands out since it allows for tracking the evolution of distinct mass transfer phenomena that contribute to the overall membrane potential drop under different current regimes [12,13].

The present work aims to evaluate the selective extraction/fractionation of four VFAs (acetic, propionic, butyric and valeric acids) via electrodialysis from a synthetic solution that simulates a fermented medium used in the PHA production. Systematic ED experiments were conducted using three commercial AEMs presenting distinct characteristics. The ED tests were performed at various cell voltages [0 V (no voltage) to 2.88 V] to evaluate the effects of the dominant transport mechanisms at underlimiting and overlimiting current regimes on the selective transport of the VFAs. Overlimiting regimes were considered herein since several authors have verified that they may reduce the membrane area, apparatus dimensions, operating time, enhance ion transport and mitigate fouling occurrence [5]. The main mass transfer mechanisms (diffusion, migration, electroconvection), water dissociation phenomenon, and transport properties of the membranes/solution systems (limiting current density and electrical resistance) were also evaluated by linear sweep voltammetry and chronopotentiometry. The occurrence of sorption was investigated in the ED tests and via chronopotentiometry evaluations.

2. Materials and methods

A simplified flowchart of the main evaluations conducted by linear sweep voltammetry, chronopotentiometry and electrodialysis is shown in Figure S1 (see supplementary material), whereas a detailed description of the materials and methods is presented below.

2.1. Electrodialysis

2.1.1. Electrodialysis system

The ED experiments were conducted using an ED-Z mini unit (Mega, Czech Republic) containing two CEMs and an AEM separated by spacers forming four compartments, as represented in Fig. 1. A Ralex CMH-PES cation-exchange membrane was present at each of the two extremities of the stack (facing the two electrodes) and the AEM under evaluation was mounted in the center, thus separating the feed solution from the receiver solution. The total effective membranes area was 64 cm^2. The ED compartments were independently connected to three external magnetically stirred reservoirs containing 250 ml (feed and receiver) and 500 ml (electrodes) of the solutions, which operated at room controlled temperature (~20 °C). The electrodes compartments (anode

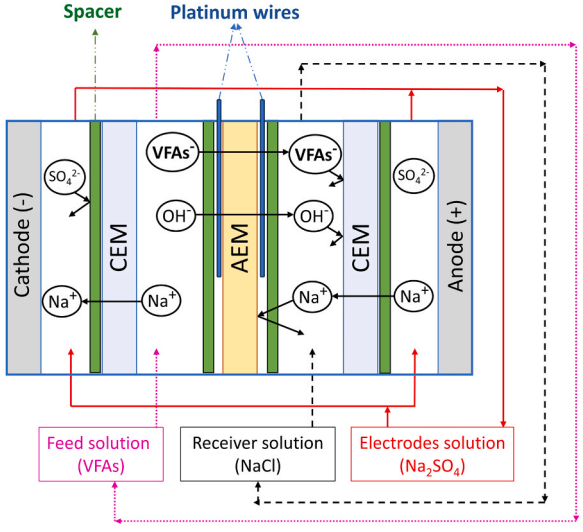

Fig. 1. – Schematic representation of the ED cell. The dotted (pink), dashed (black) and solid (red) lines connect the reservoirs containing the feed, receiver, and electrode solutions to their respective cell compartments.

and cathode) were connected to the same reservoir containing the electrodes rinse solution. Independent peristaltic pumps were used to recirculate the solutions between the ED compartments and the reservoirs at a flow rate of 13.2 L/h. The electrodes of the ED stack were connected to a potentiostat/galvanostat Autolab PGSTAT204 (Utrecht, The Netherlands), which provided the electric potential/current. Two platinum wires were placed at each surface of the AEM under evaluation for constructing the curves of linear sweep voltammetry (LSV) and chronopotentiograms (ChPs) of the membranes (AEMs)/solution systems. The experiments were conducted at least in duplicate to ensure reproducibility and the estimated relative errors between the results were below 5 %.

2.1.2. Electrodialysis operation

The ED tests were carried out in a batch potentiostatic mode. Before each test, distilled water was recirculated through all compartments/reservoirs. The experiments were carried out at several applied cell voltages, which were defined in function of the limiting current density (i_{lim}) of the membrane (Ralex)/solution system obtained by LSV. To obtain the relationships between applied cell voltage and i_{lim} of the Ralex/solution system, the LSV of the ED stack (electrodes) was also constructed, which provided the relationship between the applied voltage and the current density of the stack. Firstly, it was defined that at the cell voltages that would be applied to the ED stack, the Ralex/solution system would be investigated at 0 %, 10 %, 30 %, 50 %, 70 %, 120 %, 140 %, 160 % and 180 % of its i_{lim}. This percentage range of applied current in relation to the i_{lim} of the membrane/solution system was defined based on the percentage usually considered in ED operations, which is 70 % [14,15]. As one of the objectives of our work was to evaluate the mechanisms of the transfer of VFAs under different current conditions, several percentage values below and above 70 % (from 0 % to 180 %) were considered herein to cover both underlimiting and overlimiting current regimes. Therefore, the ED tests were conducted under 0 V (no voltage), 1.72 V, 2.22, 2.35 V, 2.45 V, 2.66 V, 2.74 V, 2.82 V, and 2.88 V, respectively.

The duration of the experiments was 7 hours. Aliquots (3 ml) were withdrawn from the feed and receiver solutions reservoirs at the beginning (after approximately 1 minute of recirculation of the working solutions, when the voltage was initially applied) and at 0.5 h, 1 h, 3 h, 5 h, 7 h for analyzing the pH and conductivity of the solutions and the VFAs concentrations.

2.1.3. Ion-exchange membranes

Three AEMs were evaluated: a heterogenous Ralex AMH-PES (Mega a.s, Czech Republic) and a Fumasep FAS-PET-130 (FuMa-Tech GmbH, Germany) and a PC200D (PCA - Polymerchemie Altmeier GmbH, Germany), which are homogeneous. Ralex and Fumasep contain quaternary ammonium as fixed functional groups, whereas PC200D contains tertiary amines in addition to the quaternary ammonium groups. The latter has been developed to allow for the transfer of ions of up to 200 Da [16]. The Ralex CMH-PES cation-exchange membrane is heterogeneous and presents sulfonic acid functional groups. Table 1 presents the main characteristics of the AEMs and CEM.

2.1.4. Solutions

The working (feed) solution was prepared with distilled water and the following VFAs at 25 mmol/L (each): acetic acid (Fisher Scientific, Loughborough, UK), propionic acid, butyric acid, and valeric acid (Acros Organics, Geel, Belgium). The solution pH was adjusted to 6 using NaOH (Fisher Scientific, Loughborough, UK) and its initial conductivity was equal to 6.2 mS/cm. As distilled water was recirculated through the ED compartments and reservoirs before each experiment and a small amount of water remained in the tubing, the actual concentration of each acid at the beginning of the experiments was approximately 23 mmol/L, the actual pH was approximately 6.15 and the conductivity was approximately 6 mS/cm.

The solution that received the VFAs (receiver) was composed of 0.1 mol/L NaCl (Panreac, Barcelona, Spain) prepared with distilled water and presented initial a conductivity of 9.6 mS/cm. The electrodes rinse solution was composed of 0.14 mol/L (20 g/L) of Na_2SO_4 (Panreac, Barcelona, Spain), prepared with distilled water and presented an initial conductivity of 17 mS/cm.

2.1.5. Analytical methods

The concentrations of the VFAs in each sample was determined by HPLC using a VWR Hitachi Chromaster chromatographer (Hitachi, Tokyo, Japan) equipped with a Pump 5160, an auto sampler 5260, a Column Oven 5310, a Diode Array Detector 5430, a RI Detector 5450, a Biorad 125–0129 30 × 4.6 mm pre-column, and an Aminex HPX-87H 300 × 7.8 mm column (0.01 M H_2SO_4 eluent, flow rate 0.6 ml/min and column temperature 60 °C). The pH and conductivity of the solutions were measured using a pH meter Sension+ pH3 (Hach, Loveland, CO, USA) and a conductivity meter (Horiba Laqua-PC1100, Japan), respectively.

2.1.6. Equations

The ED performance was evaluated in function of the percent extraction of VFAs from the feed solution and the flux of VFAs that reached the receiver solution.

The percent extraction (PE%) was calculated by Eq. 1, where $C^j_{F(t=0)}$ and $C^j_{F(t=i)}$ are the concentrations of each VFA (j) in the feed (F) solution at the initial state ($t = 0$) and at time i, respectively. Then, the ratios of percent extraction of acetic/propionic acids (PE_{Ac}/PE_{Prop}), propionic/butyric acids (PE_{Prop}/PE_{But}), acetic/valeric acids (PE_{Ac}/PE_{Val}), and the pairs of acetic+propionic and butyric+valeric acids ($(PE_{Ac}+PE_{Prop})/(PE_{But}+PE_{Val})$) were calculated for all voltages applied. These PE% ratios were the parameters used to evaluate the degree of VFAs fractionation in each tested condition: higher ratios indicate greater distances between the PE% of each VFA, which means a greater fractionation degree is obtained under such condition. It is worth mentioning that the ratio $(PE_{Ac}+PE_{Prop})/(PE_{But}+PE_{Val})$ is particularly important, as it allows for the evaluation of the transfer of the two shorter-chain VFAs (which are less desired for the production of PHAs) to the receiver solution and the retention of the two longer-chain VFAs (which are most desired for the production of PHAs) in the feed solution.

The VFAs flux (J) was calculated using Eq. (2), where $C^j_{R(t=i)}$ and

Table 1
Main characteristics of the AEMs.

	Ralex AMH-PES [17]	Fumasep FAS-PET-130 [18]	PC200D [19,20]	Ralex CMH-PES [21,22]
Heterogeneity	Heterogeneous	Homogeneous	Homogeneous	Heterogeneous
Matrix/binder	Polyester/ Polyethylene	Polyethylene terephthalate	Ethyl oxide/polyepichlorohydrin copolymer	Polyester/Polyethylene
Permselectivity - 0.5/0.1 M KCl (%)	>90	94–97	Not specified	>90
Thickness of dry membrane (mm)	0.45	0.1–0.13	0.09 ± 0.01	0.45
Ion-exchange capacity (meq/g dry membrane)	1.8	1 – 1.3	1.3 (quaternary), 0.6 (tertiary)	2.2
Water content	< 65	13–23	45	55

$C^j_{R(t=h)}$ are the concentration of each VFA (j) in the receiver solution (R) at time i and at time h (immediately before time i), respectively, V is the receiver solution volume, A_m is the membrane area and Δt is the time difference between t_i and t_h [23].

$$PE\% = \left(1 - \frac{C^j_{F(t=i)}}{C^j_{F(t=0)}}\right) \bullet 100 \quad (1)$$

$$J = \frac{\left(C^j_{R(t=i)} - C^j_{R(t=h)}\right) V}{A_m \Delta t} \quad (2)$$

The mass balance (MB%) of each VFA (j) was calculated considering its concentration in the feed and receiver solutions, the aliquots withdrawn throughout the experiments, and the theoretical volume in each reservoir (discounting the volume of each aliquot withdrawn at times i). Eqs. (3)–(5) were used for calculating MB%.

$$MB\%_{(t=\ \ i)} = \left(\frac{VFA^j mass\ \ _{(F+R+aliquots)\,(t=i)}}{VFA^j mass_{(F+R)\,(t=0)}}\right) \bullet 100 \quad (3)$$

$$VFA^j mass_{(F+R)\,(t=0)} = C^j_{F(t=0)} V_{F_{(t=0)}} + C^j_{R(t=0)} V_{R_{(t=0)}} \quad (4)$$

$$VFA^j mass_{(F+R+aliquots)\,(t=i)} = \left(C^j_{F(t=i)} \times theoretical\ \ V_{F_{(t=i)}}\right) + \left(C^j_{R(t=i)} \times theoretical\ \ V_{R_{(t=i)}}\right) + \sum_{i=0}^{i} \left[C_{(aliquots\ \ of\ \ F)_{(t=i)}} \times V_{(aliquots\ \ of\ F)_{(t=i)}}\right] + \sum_{i=0}^{i} \left[C_{(aliquots\ \ of\ \ R)_{(t=i)}} \times V_{(aliquots\ of\ \ R)_{(t=i)}}\right] \quad (5)$$

2.2. Linear sweep voltammetry

LSVs diagrams were constructed for two systems: membranes (AEMs)/solution and the ED stack (electrodes).

The LSV curves of the AEMs/solution system were obtained using two platinum wires, which were placed at each surface of the AEM under evaluation for acting as reference and sensor electrodes, respectively. The feed and receiver reservoirs were filled with the working solution containing the VFAs. Curves for solutions containing each of the VFAs separately (~23 mmol/L) and the solution containing all VFAs simultaneously were obtained (all solutions at pH 6). The following parameters were applied: scan rate of 0.008 mV/s, step of 0.008 V, final potential of 0.7 V for Ralex and 0.3 V for Fumasep and PC200D. The ohmic resistance (R_{ohm}) for each VFA was obtained by calculating the inverse of the slope of the tangent of the ohmic region of the curves. The i_{lim} values of the membranes/solution systems were determined by the Cowan-Brown method [24].

For obtaining the LSV curves of the ED stack (electrodes), the feed reservoir was filled with the working solution containing all VFAs simultaneously (pH 6), the receiver reservoir was filled with 0.1 mol/L NaCl solution, and the following parameters were applied: scan rate of 0.002 V/s, step of 0.01 V and final potential of 3.5 V.

2.3. Chronopotentiometry

ChPs were obtained for the AEMs/solution system using the same stack configuration as the LSVs, by filling both feed and receiver reservoirs with the working solution containing all VFAs simultaneously. The ChPs were obtained for the three AEMs and applying progressive current values between 0.002 – 0.4 A (0.03–6.25 mA/cm^2, respectively). The curves were obtained by 1) measuring the potential drop of the membrane/solution system for 10 seconds without applying electric current, 2) measuring the potential drop under application of current pulses for 400 seconds, and 3) measuring the potential drop during the relaxation period (200 seconds), when no current was applied.

3. Results and discussion

3.1. Linear sweep voltammetry

LSV curves were constructed for the Ralex, Fumasep and PC200D membranes (Fig. 2). As it can be observed, the curves did not show the typical three well-defined regions as a poorly defined plateau was obtained due to the intense solutions mixing [25,26]. The results of ohmic resistance for Ralex and Fumasep membranes obtained from the LSV curves are shown in Table 2, while for PC200D they were not possible to be calculated due to the oscillations verified with this membrane even within the ohmic region.

The LSV curves obtained for Ralex and Fumasep showed similar shapes especially at low current densities. According to Table 2, the R_{ohm} of Ralex/solution system for each VFA showed the following order: acetic < propionic < butyric ≤ valeric acids, which can be explained by the increasing molecular sizes of the VFAs, as smaller species tend to face less resistance to be transported through the membrane. For Fumasep, the R_{ohm} of the acids were virtually identical and lower than those of Ralex due to the homogeneity and lower thickness of the former [12]. As the current density increased, the i_{lim} of each VFA was reached. As shown in Fig. 2, the difference between the ohmic (first) and plateau (second) regions is very subtle, which hindered the precise i_{lim} determination by the intersection of the tangents relative to the first and second regions. Therefore, curves of Cowan-Brown method were constructed, which allow for a clearer visualization of i_{lim} [24] (see Figures S2 and S3 of supplementary material for the solutions containing each VFA separately and all VFAs simultaneously, respectively). Note in Figure S2 that the i_{lim} values of each VFA obtained with Ralex are very similar (~ 1.5 mA/cm^2), which can be explained by their identical charge and similar molecular size. For Fumasep, although the Cowan-Brown curves did not show a clear peak (minimum point), one can see that the i_{lim} values of each VFA are also similar. According to Fig. 2, at high current densities (above approximately 1.5 mA/cm^2), the curves for both Ralex and Fumasep with the solutions containing each VFA separately showed typical oscillations in the potential drop due to the dominance of overlimiting mass transfer phenomena, such as electroconvection, gravitational convection and/or water dissociation at the solution/membrane interface.

The LSV curves obtained for Ralex and Fumasep membranes with the solution containing all VFAs simultaneously, presented more than one inflection point related to the depletion of the VFAs due to concentration polarization [27]. As shown in the Cowan-Brown curves present in Figure S3 (see supplementary material), two i_{lim} values were obtained for Ralex and Fumasep with the solution containing all VFAs: 0.88 mA/cm^2 and 2.5 mA/cm^2 for Ralex, and 1.4 mA/cm^2 and 2.5 mA/cm^2 for Fumasep. The similarity between the LSVs (Fig. 2) of the acetic/propionic and butyric/valeric pairs and the presence of two i_{lim} peaks (Figure S3) indicate that these VFA pairs are depleted simultaneously during concentration polarization. For PC200D, only one peak related to the i_{lim} (1.4 mA/cm^2) can be clearly seen in the Cowan-Brown curve since intense oscillations were verified, which hindered the determination of other i_{lim} values. Considering the above-mentioned, the i_{lim} of the membrane/solution systems considered herein to define the voltages applied to the ED tests was 2.5 mA/cm^2, which is the i_{lim} value obtained for both Ralex and Fumasep membranes. As the curves for the solution containing all VFAs showed multiple inflection points, the R_{ohm} values were not determined for this solution. Oscillations under high current densities (> 3 mA/cm^2) were also observed for both Ralex and Fumasep with the solution containing all VFAs simultaneously, as expected.

According to Fig. 2c, the LSV curves obtained for PC200D showed a very different behavior from Ralex and Fumasep since intense

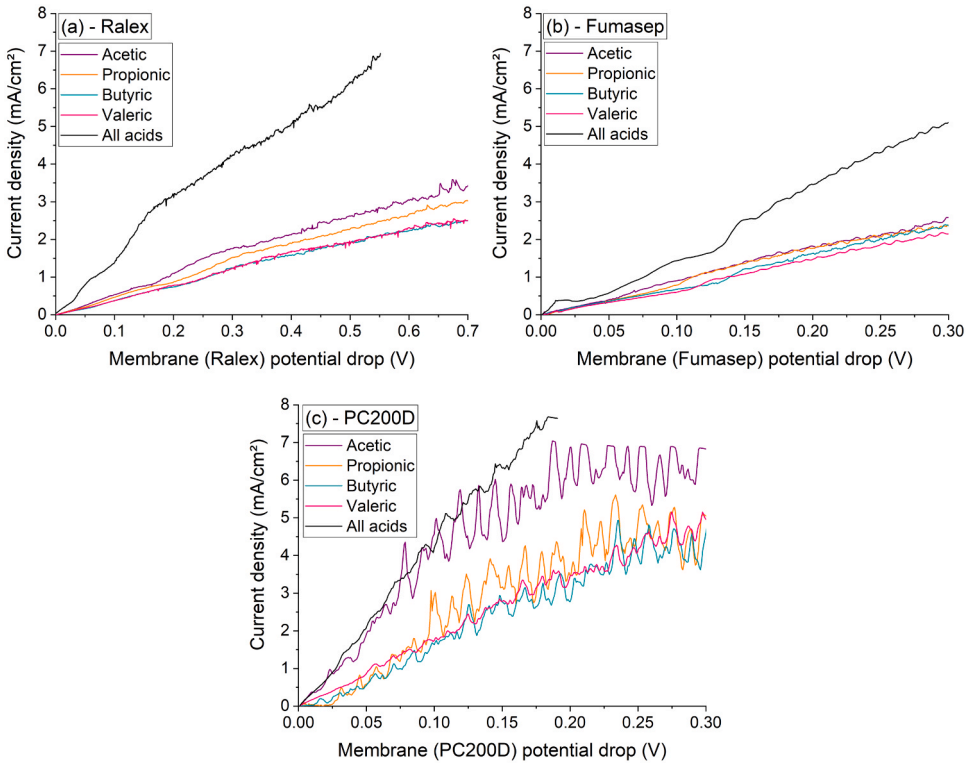

Fig. 2. – Representative LSVs of the AEMs/solution system for (a) Ralex, (b) Fumasep and (c) PC200D. The solutions contained each VFA separately and all VFAs simultaneously at initial pH 6.

Table 2
Ohmic resistance of the AEMs (Ralex and Fumasep)/solution systems obtained from the LSV curves shown in Fig. 2.

	Ralex		Fumasep	
	R_{ohm} (Ω. cm^2)	Standard deviation*	R_{ohm} (Ω. cm^2)	Standard deviation**
Acetic acid	11.7	0.3	8.2	0.1
Propionic acid	13.4	0.2	8.3	0
Butyric acid	16.6	0.1	8.4	0.1
Valeric acid	17.0	0.1	9.1	0.3

* Curves analyzed for the Ralex: acetic acid (4), propionic acid (4), butyric acid (5), valeric acid (2).
** Curves analyzed for the Fumasep: acetic acid (3), propionic acid (2), butyric acid (3), valeric acid (3).

oscillations with large amplitudes were verified especially under high current densities. This behavior was not expected since the oscillations occur less intensely even at low current densities, which made impossible the determination of R_{ohm}.

These differences between the LSV curves of the three membranes, especially the intensity and amplitude of the oscillations verified for the PC200D, can be explained by the different type and degree of hydrophobicity of their functional groups, which is the main surface property that affects overlimiting mass transfer [28]. In this case, the differences in the functional groups of the membranes affected the intensity of each overlimiting mass transfer mechanism, such as electroconvection and water dissociation, that took place at each membrane, affecting the shapes of their LSVs. While the functional groups of Ralex and Fumasep are composed of quaternary ammonium, those of PC200D are composed of quaternary ammonium and tertiary amines [16]. On one hand, it is well known that tertiary amines exhibit a higher catalytic activity to the water dissociation reaction than the quaternary ammonium groups [29]. On the other hand, tertiary amines are more hydrophobic than quaternary amines [30,31], thus favoring earlier occurrence of electroconvection phenomena with larger vortices (higher amplitudes) [11, 32]. Therefore it is expected that these phenomena are strongly competitive at the PC200D and their simultaneous occurrence at this membrane would be favored by its relatively low thickness (Table 1) since the membrane functional groups would become more exposed to the membrane/solution interface [28]. It is worth noting that the oscillations amplitude varies strongly in function of the VFA type (compare the curves for acetic and valeric acids). It is known that an ion with a bigger hydrated radius and higher hydrophobicity tends to favor electroconvection and disfavor water dissociation [32,33]. Among the VFAs tested herein, acetic acid has the lowest molecular size and hydrophobicity degree [34], which means that it would favor water dissociation occurrence. As the largest oscillations amplitude was verified for acetic acid and the lowest one was verified for valeric acid, it could be suggested that the intense oscillations of the curves are mainly associated with the water dissociation reaction. This will be also discussed in the chronopotentiometry results section (Section 3.2). Lastly, Fig. 2(c) additionally shows that the curve of acetic acid is very distant from the other VFAs and very close to the curve constructed with the solution containing all acids, showing lower electrical ohmic resistance due to its more vertical slope. This can be explained by the lower size and higher hydrophilic nature of acetic acid and, therefore its preferential transport through the membrane. As such a difference between the VFAs was not verified for Ralex and Fumasep, Fig. 2 suggests that PC200D strongly favors the transport of acetic acid while the other VFAs are transported at a considerably lower rate, which was confirmed by the results obtained in the ED experiments (Section 3.3).

The LSV curve obtained for the ED stack (electrodes) with Ralex membrane is shown in Figure S4 (see supplementary material). This curve was used for determining the voltage values that would be applied in the ED tests in function of the $i/i_{\lim}$ ratios of the Ralex/solution system, as described in Section 2.1.2.

3.2. Chronopotentiometry

ChPs at several applied current densities (0.03 mA/cm^2 – 6.25 mA/cm^2) were obtained for each membrane using the solution containing all VFAs simultaneously at initial pH 6. The results are shown in Fig. 3.

The ChPs obtained for each membrane showed distinct behaviors. For all membranes, the potential drop maintained constant over time when low values of current density were applied (see 0.03 mA/cm^2) indicating that the VFAs transfer was governed by diffusion/migration [12]. As the applied current increased, the initial potential drop (E_Ω – indicated in Fig. 3a) increased, which is related to the ohmic contribution of the membrane/solution system when the membrane was not yet under the effect of intense concentration polarization [13]. This property was similar for all membranes, showing values close to zero for low currents, as expected, and between 0.05 V – 0.08 V for higher currents.

As the current density increased, an inflection point appeared, and the potential drop measured over time increased strongly due to the concentration polarization occurrence. Then, a quasi-steady state condition was reached due to the dominance of overlimiting transport mechanisms [12,13,32]. It is worth noting that this increase in potential drop occurred in a very short time for all membranes, without showing the typical inflection point related to the reduction in concentration when the membrane/solution system reaches the concentration polarization condition. Therefore, when current density values greater than i_{lim} are applied, the time during which the VFAs are transferred by electro-diffusion, before being transferred by overlimiting mechanisms, is extremely short or even non-existent [12].

The region of quasi-steady state condition after the concentration polarization occurrence showed different behaviors for each membrane. The potential drop values measured for Ralex were considerably higher than for Fumasep and PC200D under the same current densities (for example 0.43 V, 0.23 V and 0.20 V, respectively, under 6.25 mA/cm^2). This indicates a greater overlimiting resistance of Ralex, which can be explained by its heterogeneity and the consequent tortuous counter-ion pathway [35].

For Ralex, the curves under moderate current values showed subtle oscillations over time, and the intensity of the oscillations increased with increasing applied current density (compare 1.25 mA/cm^2 to 6.25 mA/cm^2). Thus, under high current densities, the VFAs transfer through Ralex was governed by electroconvection [36], whereas the occurrence of intense water dissociation was not verified for this membrane. Differently, Fumasep showed intense oscillations of potential drop even at moderate current density values (0.78 mA/cm^2) and this increased with current density. Furthermore, after the rapid increase in potential drop during concentration polarization under high current densities, the potential drop reached a peak (maximum point) between 0 – 15 seconds and then reduced until the quasi-steady state condition was reached (indicated at Fig. 3b). This maximum point is generally associated with the occurrence of gravitational convection or water dissociation on the membrane surface. As gravitational convection occurs in more concentrated solutions [37], the maximum point shown in the present work appeared due to the water dissociation phenomenon.

The curves for PC200D were similar to those obtained for Fumasep, but the curves of the former did not show oscillations under moderate current densities. Note that the oscillations with the PC200D started to appear at 1.88 mA/cm^2 and intensified with the increase in current density. Potential drop peaks (maximum point) between 0 – 15 seconds were also verified for this membrane, indicating the occurrence of water dissociation. The potential drop of the curves under high current densities (greater than 2.5 mA/cm^2) did not reach a quasi-steady state condition, showing a continuous increase until the current application was interrupted (indicated in Fig. 3(c)). This continuous increase in E_m can be explained by the intense water dissociation occurrence at the diluate interface of PC200D, the consequent transfer of the formed OH^- ions to the concentrated compartment, and the Donnan exclusion of protons at the membrane diluate interface [38]. Thus, the accumulated protons shifted the chemical equilibrium of the VFA species, which became protonated (pKa ~4.8). These uncharged species accumulated

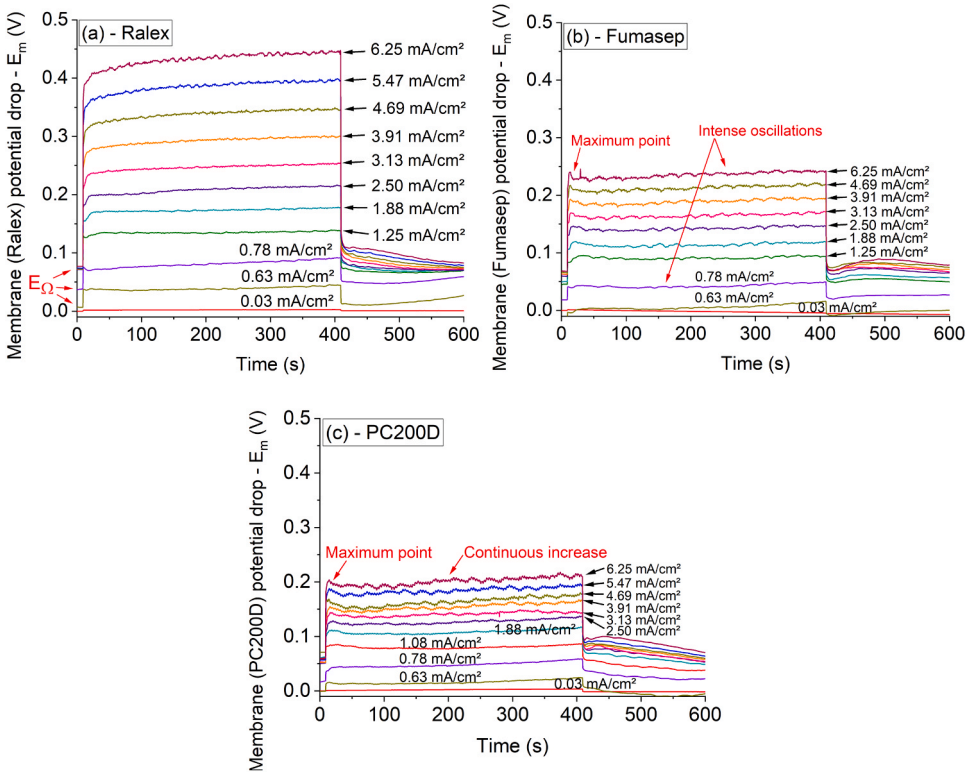

Fig. 3. – Representative ChPs of the membrane/solution systems obtained for (a) Ralex, (b) Fumasep and (c) PC200D. The solution was composed of all VFAs at initial pH 6.

at the diluate side of the PC200D and caused the continuous increase of its resistance, as shown in Fig. 3c. The oscillations of potential drop after the maximum point for PC200D were more intense than those of Fumasep, indicating that the overlimiting mechanisms occurred more intensely at the former. As already discussed, this can be explained by the presence of tertiary amines in PC200D and agrees with the LSVs shown in Fig. 2c. Besides, the maximum point of E_m and intense oscillations for PC200D indicate the occurrence of electroconvection simultaneously to water dissociation, which supports the discussion on the competition of these phenomena (Section 3.1).

Lastly, the relaxation section of the membrane/solution systems, after interrupting the electric current application, showed a similar behavior for all membranes. After applying low current densities, the potential drop during relaxation remained close to zero, as expected. As the applied current density increased, the potential drop during relaxation dropped to a non-zero value (between approximately 0.05 V and 0.1 V for all membranes) and remained practically constant, showing a very slow decrease over time. This is related to the non-ohmic resistance of the membrane system, which depends strongly on the DBL thickness [39], and can be explained by the changes in VFAs concentration at the diluate and concentrated interface of the membranes after each current pulse application.

3.3. Electrodialytic separation

ED experiments were conducted under distinct cell voltage values [0 V (no voltage), 1.72 V, 2.22 V, 2.35 V, 2.45 V, 2.66 V, 2.74 V, 2.82 V, 2.88 V] and their performance was evaluated by calculating the percent extraction and flux of VFAs.

3.3.1. Percent extraction

Figs. 4–6 show the results of percent extraction (PE%) as a function of time (0 – 7 h) for the ED tests conducted at 0 V (no voltage applied), 1.72 V, 2.35 V, 2.45 V, 2.66 V, 2.88 V with Ralex, Fumasep and PC200D membranes, respectively. The results for voltages of 2.22 V, 2.74 V and 2.82 V showed similar behaviors and are present in Figures S5-S7 (see supplementary material).

To support the discussions on the selectivity of each VFA transport, the ratios of percent extraction of acetic/propionic acids (PE_{Ac}/PE_{Prop}), propionic/butyric acids (PE_{Prop}/PE_{But}), acetic/valeric acids (PE_{Ac}/PE_{Val}) and the pairs of (acetic+propionic)/(butyric+valeric) acids ($PE_{Ac}+PE_{Prop}$)/($PE_{But}+PE_{Val}$) were calculated for all voltages applied. The greater the ratio, the greater the fractionation degree of the VFAs pairs. The results for the samples withdrawn at times 0.5 h, 3 h and 7 h are shown in Table 3, whereas the complete table containing the results for all samples withdrawn (0 h, 0.5 h, 1 h, 3 h, 5 h, 7 h) is shown in Table S1 (see supplementary material).

According to Figs. 4–6, increasing the cell voltage increased the percent extraction for all membranes at all times evaluated, as expected, but the membranes showed different behaviors. The overall percent extraction of all acids obtained with Fumasep were considerably higher than with Ralex, especially under no (0 V) or medium (1.72 V – 2.45 V) voltages. This greater transport of ions through the homogeneous membrane was expected because of its lower thickness and, consequently, lower electrical resistance [40]. Under high voltages (2.45 V – 2.88 V), Ralex and Fumasep membranes showed similar performances, indicating that the alteration of the dominant ion transport mechanism from diffusion/migration to the overlimiting suppressed the effects of membrane homogeneity. Under all voltages applied (0 V – 2.88 V), PC200D showed percent extraction values of acetic acid practically identical to those of Fumasep. For propionic acid, the values of PE% obtained with PC200D were slightly lower than those with Fumasep, while for butyric and valeric acids the PE% values were considerably lower.

The PE% values of the VFAs obtained with Ralex and Fumasep showed the following order: acetic > propionic > butyric = valeric, while for PC200D the order was acetic > propionic > butyric > valeric. This behavior was partially expected since the lower the size of a specie, the faster is its transport across conventional ion-exchange membranes. On the other hand, only PC200D allows for the fractionation of butyric and valeric acids.

According to Table 3, Fumasep showed a slightly greater selectivity in the separation of acetic and propionic acids compared to Ralex in a short time (PE_{Ac}/PE_{Prop} = 1.1–1.3), while PC200D showed a much

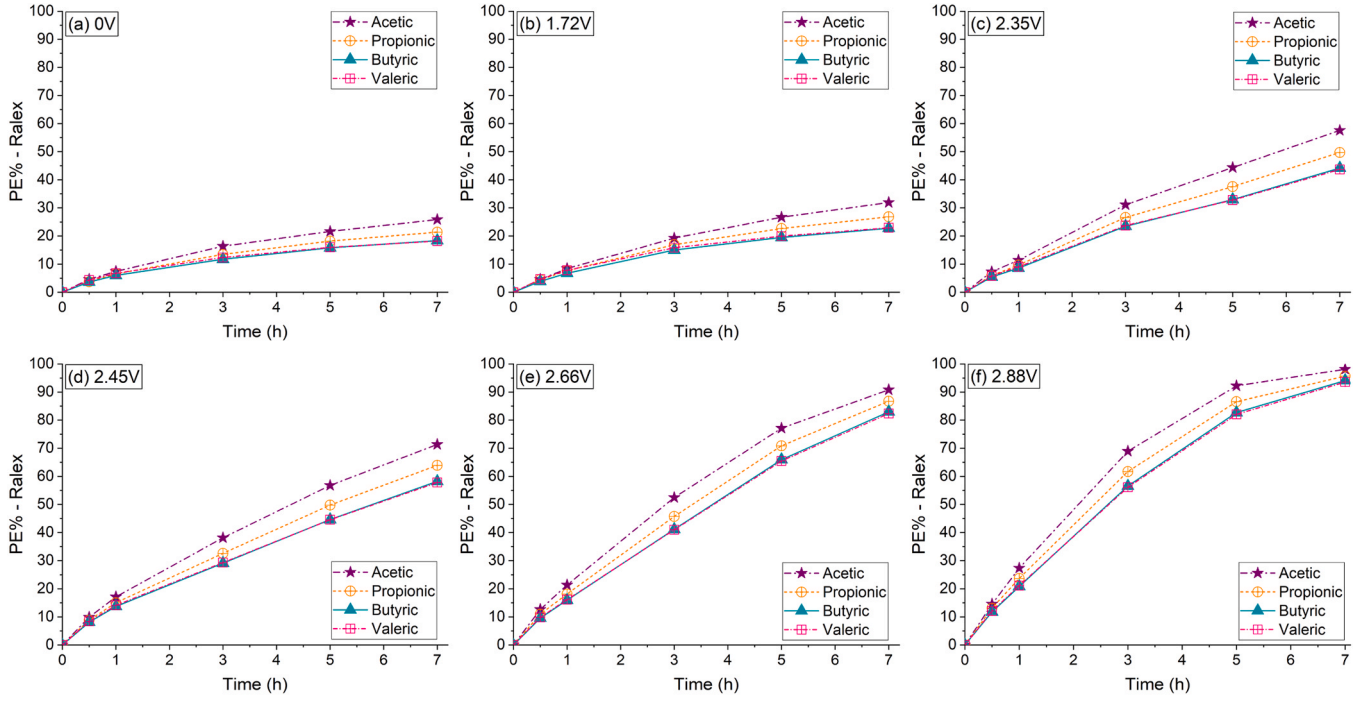

Fig. 4. – Representative PE% obtained with the Ralex membrane under (a) 0 V, (b) 1.72 V, (c) 2.35 V, (d) 2.45 V, (e) 2.66 V and (f) 2.88 V throughout 7 hours of electrodialysis.

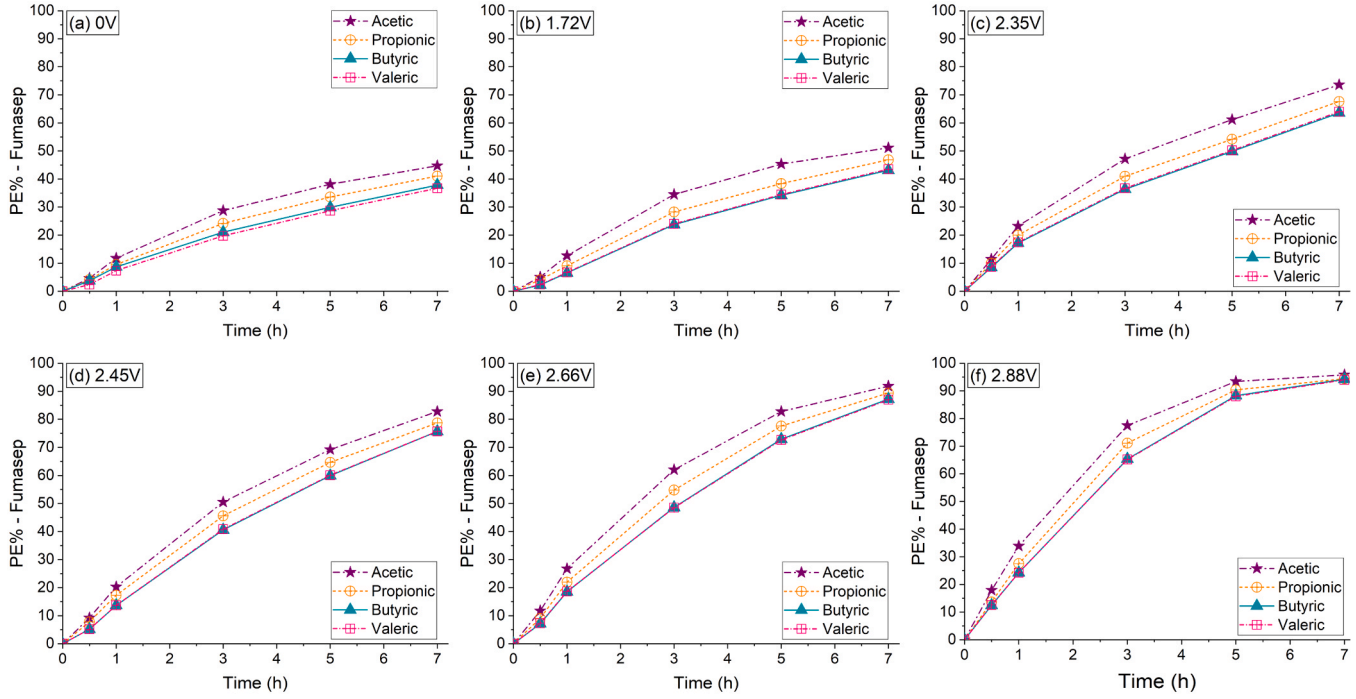

Fig. 5. – Representative PE% obtained with the Fumasep membrane under (a) 0 V, (b) 1.72 V, (c) 2.35 V, (d) 2.45 V, (e) 2.66 V and (f) 2.88 V throughout 7 hours of electrodialysis.

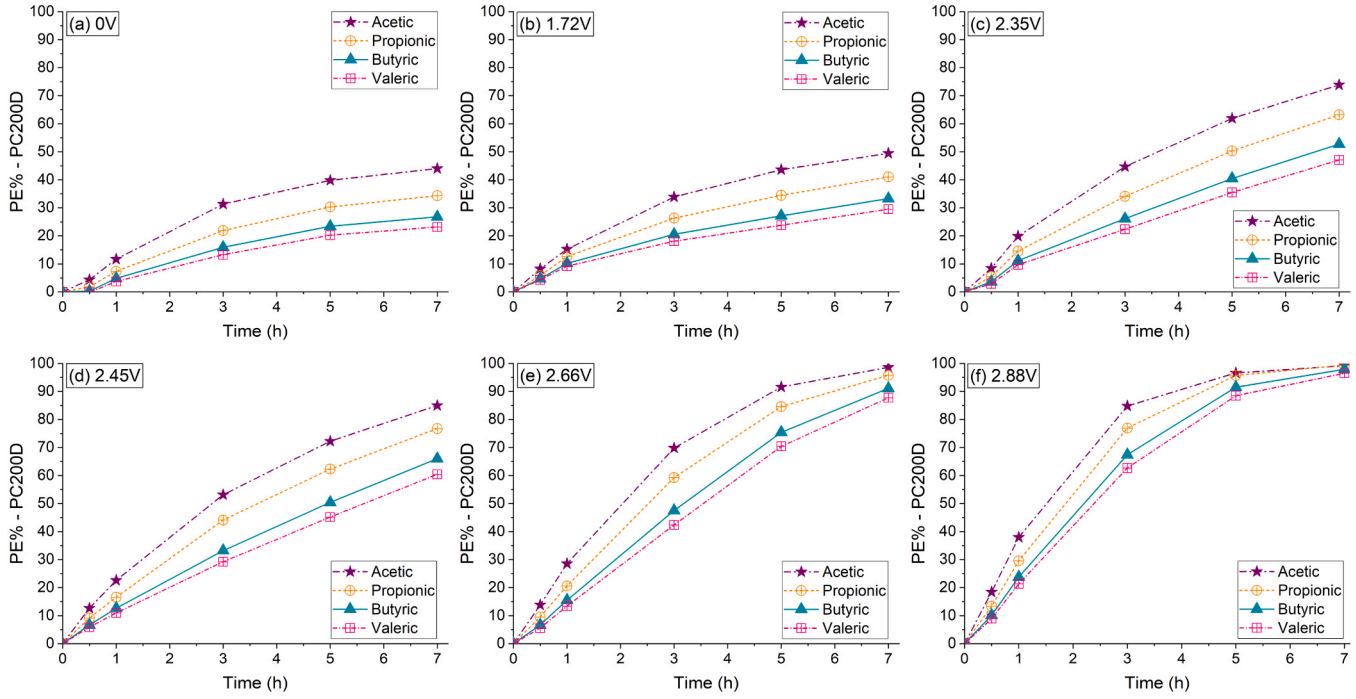

Fig. 6. – Representative PE% obtained with the PC200D membrane under (a) 0 V, (b) 1.72 V, (c) 2.35 V, (d) 2.45 V, (e) 2.66 V and (f) 2.88 V throughout 7 hours of electrodialysis.

greater selectivity for these acids especially when no current was applied ($PE_{Ac}/PE_{Prop} = 2.4$). For medium-long operating times (3 h and 7 h), the separation of acetic and propionic acids with Ralex and Fumasep was similar ($PE_{Ac}/PE_{Prop} = 1.0–1.3$), while for PC200D the distance between the curves remained greater than for the other membranes ($PE_{Ac}/PE_{Prop} = 1.0–1.4$). Regarding the separation of propionic and butyric acids, Ralex and Fumasep showed similar ratios of PE_{Prop}/PE_{But} for all times (1.0 – 1.3), while for PC200D the ratio was 6.6 without voltage application and short time, and between 1.0 – 1.4 for the other voltages and times. The ratio of acetic and valeric acids (PE_{Ac}/PE_{Val}) was 1.1 – 1.3 for Ralex, 1.2 – 2.0 for Fumasep and 1.4 – 4.2 for PC200D. Lastly, the percent extraction ratios for the acetic+propionic and butyric+valeric pairs ($PE_{Ac}+PE_{Prop})/(PE_{But}+PE_{Val}$) exhibited a similar behavior to the other ratios mentioned, indicating that the PC200D allows for the

Table 3
Percent extraction ratios of PE_{Ac}/PE_{Prop}, PE_{Prop}/PE_{But}, PE_{Ac}/PE_{Val} and $(PE_{Ac}+PE_{Prop})/(PE_{But}+PE_{Val})$ obtained in the electrodialysis tests under distinct voltages applied.

		PE% ratios											
		Ralex				Fumasep				PC200D			
Cell voltage (V)	Time (h)	Ac/ Prop	Prop/ But	Ac/ Val	(Ac+Prop)/ (But+Val)	Ac/ Prop	Prop/ But	Ac/ Val	(Ac+Prop)/ (But+Val)	Ac/ Prop	Prop/ But	Ac/ Val	(Ac+Prop)/ (But+Val)
0	0.5	1.2	1.0	1.1	1.0	1.3	1.1	2.0	1.3	2.4	6.6	4.2	4.7
	3	1.2	1.1	1.3	1.2	1.2	1.1	1.5	1.3	1.4	1.4	2.4	1.8
	7	1.2	1.2	1.4	1.3	1.1	1.1	1.2	1.2	1.3	1.3	1.9	1.6
1.72	0.5	1.0	1.1	1.0	1.1	1.2	1.1	1.3	2.0	1.4	1.2	1.9	1.4
	3	1.1	1.1	1.2	1.2	1.1	1.1	1.3	1.3	1.3	1.3	1.9	1.6
	7	1.2	1.2	1.4	1.3	1.0	1.1	1.1	1.1	1.2	1.2	1.7	1.4
2.22	0.5	1.2	1.1	1.2	1.1	1.2	1.2	1.5	1.3	1.3	1.2	1.7	1.5
	3	1.2	1.1	1.4	1.3	1.2	1.2	1.4	1.3	1.3	1.3	2.1	1.7
	7	1.2	1.2	1.4	1.3	1.1	1.1	1.2	1.2	1.2	1.2	1.7	1.5
2.35	0.5	1.2	1.1	1.3	1.2	1.1	1.2	1.3	1.2	1.5	1.5	2.9	2.1
	3	1.2	1.1	1.3	1.2	1.2	1.1	1.3	1.2	1.3	1.3	2.0	1.6
	7	1.2	1.1	1.3	1.2	1.1	1.1	1.1	1.1	1.2	1.2	1.6	1.4
2.45	0.5	1.1	1.1	1.2	1.1	1.2	1.1	1.3	1.6	1.4	1.4	2.2	1.7
	3	1.2	1.1	1.3	1.2	1.1	1.1	1.2	1.2	1.2	1.3	1.8	1.6
	7	1.1	1.1	1.2	1.2	1.0	1.0	1.0	1.1	1.1	1.2	1.4	1.3
2.66	0.5	1.2	1.1	1.3	1.2	1.3	1.3	1.6	1.4	1.5	1.4	2.5	1.9
	3	1.1	1.1	1.3	1.2	1.1	1.1	1.3	1.2	1.2	1.2	1.6	1.4
	7	1.0	1.0	1.1	1.1	1.0	1.0	1.1	1.0	1.0	1.1	1.1	1.1
2.74	0.5	1.2	1.2	1.3	1.3	1.2	1.2	1.3	1.3	1.3	1.3	1.8	1.5
	3	1.1	1.1	1.3	1.2	1.1	1.1	1.2	1.1	1.1	1.2	1.5	1.4
	7	1.0	1.0	1.1	1.0	1.0	1.0	1.0	1.0	1.0	1.0	1.1	1.1
2.82	0.5	1.3	1.2	1.4	1.3	1.3	1.3	1.6	1.4	1.3	1.3	1.9	1.6
	3	1.1	1.1	1.3	1.2	1.1	1.1	1.2	1.1	1.1	1.2	1.4	1.3
	7	1.0	1.0	1.1	1.0	1.0	1.0	1.0	1.0	1.0	1.0	1.0	1.0
2.88	0.5	1.1	1.1	1.2	1.2	1.3	1.1	1.4	1.3	1.4	1.3	2.1	1.7
	3	1.1	1.1	1.2	1.2	1.1	1.1	1.2	1.1	1.1	1.1	1.4	1.2
	7	1.0	1.0	1.0	1.0	1.0	1.0	1.0	1.0	1.0	1.0	1.0	1.0

transfer of a large portion of acetic and propionic acids to the receiver solution while retaining part of the butyric and valeric acids in the feed solution especially in short times and low voltages. This behavior verified for the PC200D differed considerably from that of the Ralex and Fumasep membranes. With the PC200D, percent extractions of acetic and propionic acids between 70 % and 77 % and 60 %-67 % were obtained, respectively, achieving a $(PE_{Ac}+PE_{Prop})/(PE_{But}+PE_{Val})$ ratio of 1.4 under 2.35 V (7 hours), 2.45 V (5 hours), 2.66 V (3 hours), and 2.74 V (3 hours).

Overall, the membranes showed a reduction in the PE_{Ac}/PE_{Prop}, PE_{Prop}/PE_{But}, PE_{Ac}/PE_{Val} and $(PE_{Ac}+PE_{Prop})/(PE_{But}+PE_{Val})$ ratios with increasing voltage (for a defined time) especially at longer times, which can be explained by the alteration of the dominant ion transport mechanism at underlimiting and overlimiting current regimes. This indicates that voltage values greater than 2.88 V are not recommended for the ED application evaluated herein. The results obtained for all membranes indicate that ion transport governed by diffusion/migration (without application of voltage) allows for a more selective separation between the acids, which is most notable for PC200D. In this case, ion transport occurs mainly due to differences in species concentration in the diluted/concentrated compartments and is virtually not influenced by their charges, which are identical for all VFAs evaluated here (diffusion coefficients in water at infinite dilution of $1.089{\cdot}10^{-5}$ cm^2/s, $0.953{\cdot}10^{-5}$ cm^2/s, $0.868{\cdot}10^{-5}$ cm^2/s, and $0.593{\cdot}10^{-5}$ cm^2/s for acetate, propionate, butyrate and valerate anions, respectively [41,42]). When voltage is applied, ion transport is primarily governed by electromigration, and in this case, the identical charges of the species result in ions being extracted similarly. The difference between the values of PE_{Ac}/PE_{Prop}, PE_{Prop}/PE_{But}, PE_{Ac}/PE_{Val} and $(PE_{Ac}+PE_{Prop})/(PE_{But}+PE_{Val})$ obtained in tests conducted without and with potential application, especially for PC200D at a short operating time (0.5 h), indicates that the effects of electric charge on ion transfer by electromigration is more intense at membranes containing tertiary amines than at those presenting only quaternary ammonium groups. As the applied voltage increased from 1.72 V to 2.88 V, the ratios of PE% decreased, especially at medium (3 h) and longer (7 h) times because of the effects of overlimiting mechanisms. As mentioned, the intense occurrence of water dissociation at the diluate side of PC200D, which was verified in the LSVs, ChPs, and pH profiles that will be shown in Section 3.3.3, led to the formation of protonated (uncharged) VFAs at the membrane surface. In this case, the transport of VFAs by electromigration may have ceased to be relevant and became governed by diffusion. Some authors have evaluated the selective separation of VFAs using adsorbents and noted that those materials containing quaternary ammonium allow for strong

adsorption by anion exchange, while tertiary amines predominantly adsorb uncharged VFAs due to hydrophobic interactions [3,4]. Thus, in the present study, the formation of uncharged species under intense water dissociation at PC200D may have intensified the transport of species across this membrane by diffusion.

All membranes showed a reduction trend in the ratios of PE_{Ac}/PE_{Prop}, PE_{Prop}/PE_{But}, PE_{Ac}/PE_{Val}, and $(PE_{Ac}+PE_{Prop})/(PE_{But}+PE_{Val})$ with increasing time (for a defined cell voltage), especially under high voltages. The lower fractionation degree at longer times occurred because, in this case, the smallest ions have already been transferred to the concentrated compartment. Thus, the competition between smaller and larger ions decreased, allowing the larger ones to migrate more intensely through the membrane despite their larger size. This is particularly noticeable for PC200D, indicating that the concentration ratio of species of different sizes present in the diluate solution strongly affects their separation.

Our results showing the possibility of fractionating the VFAs under certain time frame and cell voltage conditions, especially with the PC200D, differ from the results obtained by Tao et al. [43], who found a nearly identical percent extraction of acetic/butyric and propionic/butyric acids in an electrodialytic separation using the PC SA membrane (PCCell GmbH, Germany). Jones et al. [6] also obtained percent extractions of acetic and butyric acids very close to each other, but did not specify the membrane that was used. Brown et al. [7] evaluated the electrodialytic separation of VFAs and verified that the polytetrafluoroethylene membrane does not have any selectivity towards the acids evaluated herein, showing identical percent extractions. Lastly, the results obtained herein also differ from those showed by Scoma et al. al. [8], who obtained a separation factor of only 1.14 for acetic and butyric acids and 1.1 for acetic and propionic acids using Neosepta AMX membrane (Astom Corporation, Japan).

3.3.2. *Flux and mass balances*

The evaluation of the reach of VFAs to the concentrated compartment was performed by calculating their flux. Figs. 7–9 present the flux results over time under cell voltages of 0 V, 1.72 V, 2.35 V, 2.45 V, 2.66 V, 2.88 V obtained with Ralex, Fumasep, and PC200D membranes, respectively. The results for all voltages tested (0 V – 2.88 V) are shown in Figures S8 – S10 (see supplementary material).

As expected, the flux curves for each acid transported through each membrane showed a similar trend to the percent extraction: acetic > propionic > butyric ≥ valeric. The distances between the curves also follows similar behaviors to the PE% values, which are different for each membrane and decrease over time. Note that at longer times, especially for Fumasep and PC200D under high potentials, the flux of VFAs that have a larger size (butyric and valeric acids) became greater than the flux of acetic and propionic acids, which can be explained by the lower competition between small and large ions when transported through the membrane, as discussed in Section 3.3.1. For Ralex, an unexpected behavior of the flux values over time was observed. Note that the flux increased from short times, remained constant, and then decreased, which is more evident under higher applied voltages. This indicates that the flux values of ions reaching the concentrated compartment were lower than the expected, especially at short times, which may have occurred due to ion sorption in the membrane phase. To shed light on this phenomenon, the mass balance of the species throughout the tests was estimated for all voltages applied, and the results are present in Table S2 (see supplementary material). It is worth mentioning that values slightly above 100 % (101 % – 104 %) are due to intrinsic deviations in the chemical analysis.

According to Table S2, the mass balance remained at 100 % throughout the experiments (0 – 7 h) with all membranes when no voltage was applied. For Fumasep and PC200D, the mass balance closure gradually decreased over time (up to 85 %) especially under high voltages (greater than 2.35 V). This may have occurred because, at longer times and high voltages, two opposing driving forces acted on the VFAs: the electromigration force associated with electroconvection towards the concentrated compartment and the back diffusion force towards the diluate compartment [44]. Thus, part of the VFAs were retained at/in the membranes. Besides, the intense water dissociation at these membranes (confirmed in the ChPs and pH profiles that will be shown in the next section) led to the decrease of pH at the membranes diluate side and bulk solution, where part of the acids were present in their free form. The high concentration of free VFAs may have been responsible for their

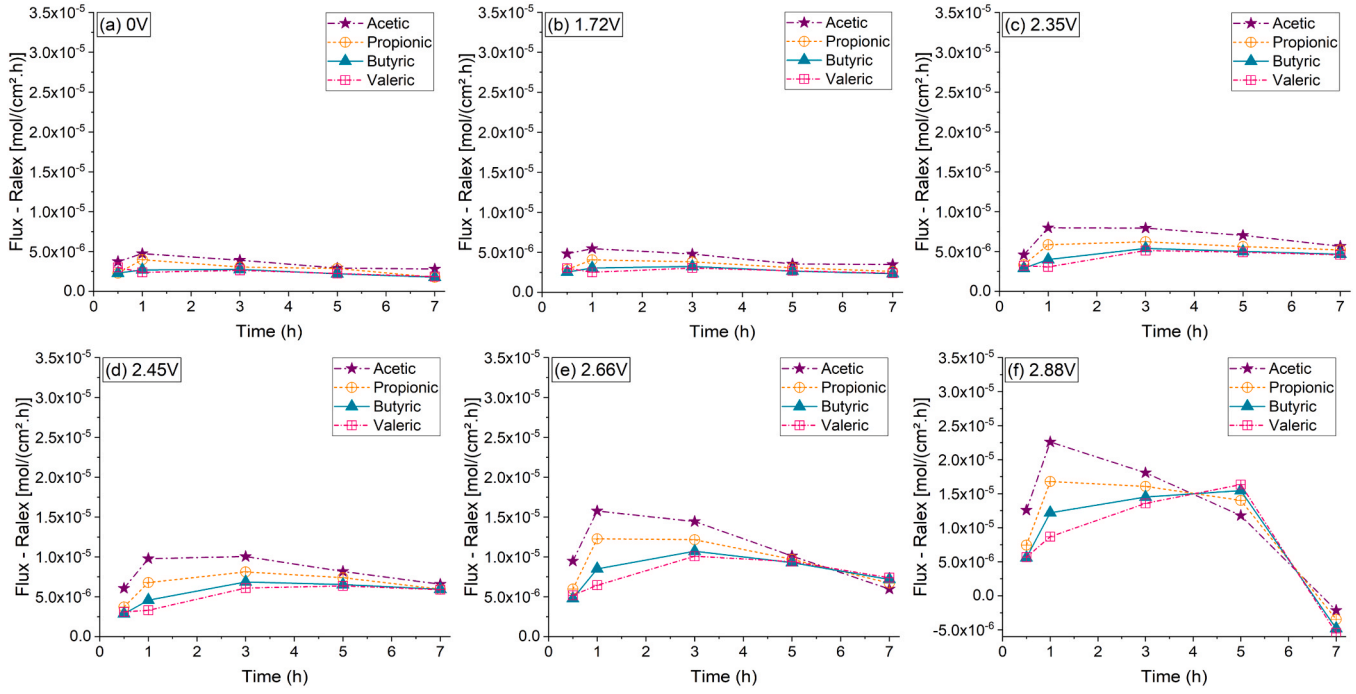

Fig. 7. – Representative flux obtained with the Ralex membrane under (a) 0 V, (b) 1.72 V, (c) 2.35 V, (d) 2.45 V, (e) 2.66 V and (f) 2.88 V throughout the electrodialysis.

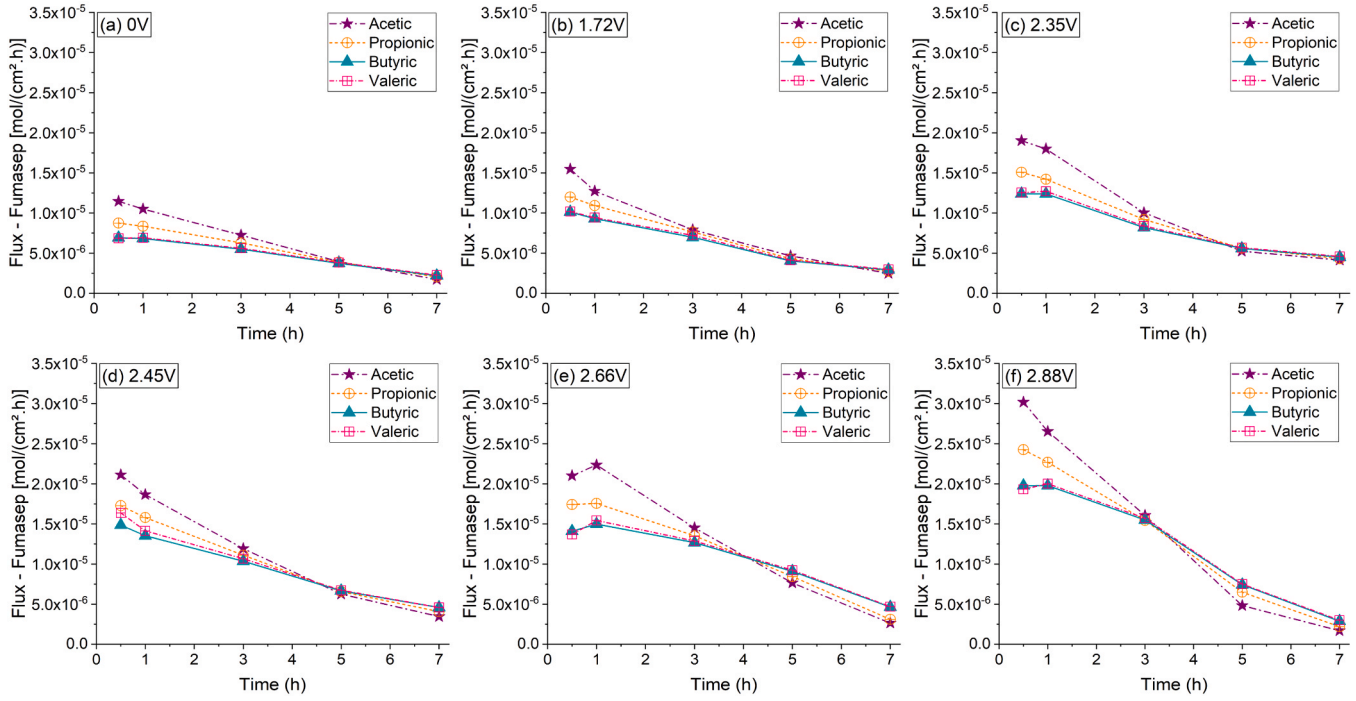

Fig. 8. – Representative flux obtained with the Fumasep membrane under (a) 0 V, (b) 1.72 V, (c) 2.35 V, (d) 2.45 V, (e) 2.66 V and (f) 2.88 V throughout the electrodialysis.

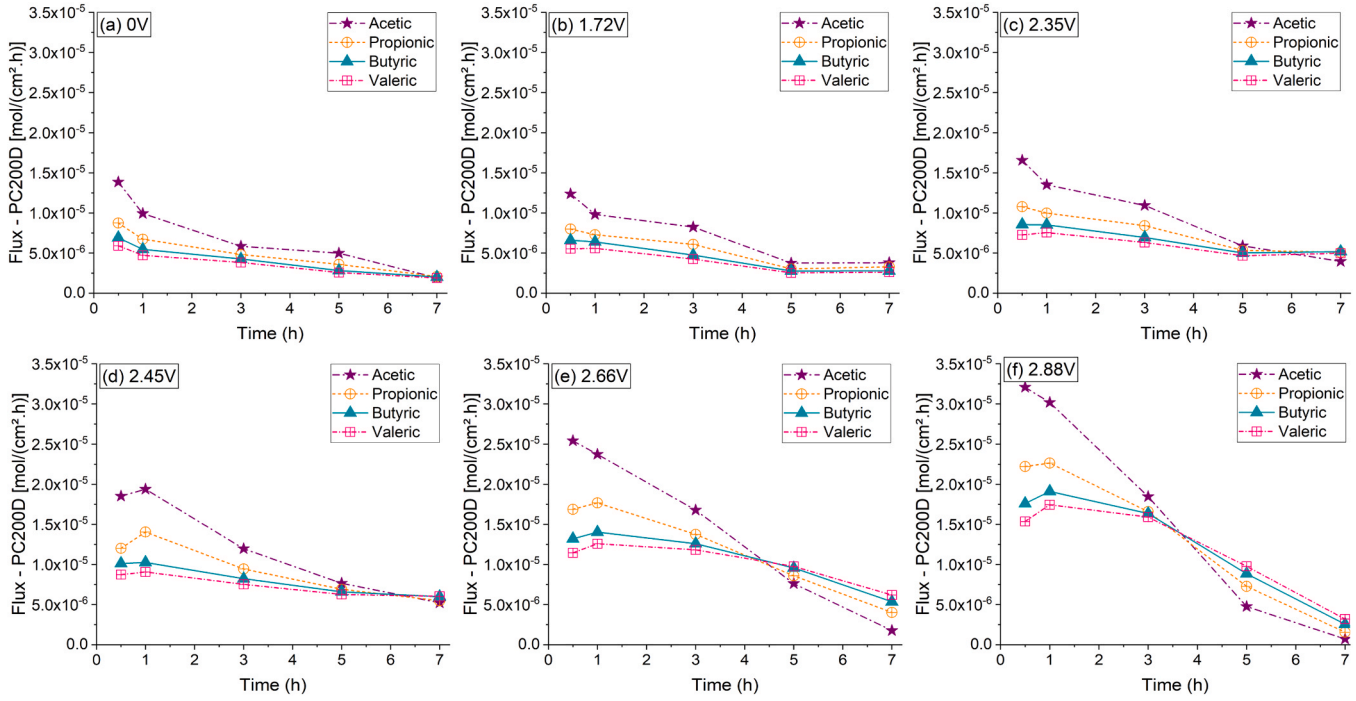

Fig. 9. – Representative flux obtained with the PC200D membrane under (a) 0 V, (b) 1.72 V, (c) 2.35 V, (d) 2.45 V, (e) 2.66 V and (f) 2.88 V throughout the electrodialysis.

loss by evaporation due to their high volatility [3,43], which can also explain the decrease in mass balance closure for Fumasep and PC200D membranes. The Ralex membrane showed a different behavior. Note that a strong reduction in the mass balance was observed for this membrane (up to 72 %) even at short times (0.5 h), reaching considerably lower values of MB% than the other membranes. Besides, there is a clear relationship between ion size and sorption intensity for Ralex: the smaller the ion, the more intense the sorption. The intense sorption in Ralex can be explained by its greater thickness and the presence of clusters of ion exchange sites as it is a heterogeneous membrane. Several works on sorption have been published on literature, which were conducted using single salt solutions, pesticides or pharmaceuticals [45,46]. Some of these works showed that the membrane thickness strongly influences ion sorption, but only few works on VFAs sorption have been

published. As sorption occurrence may reduce the membrane conductivity and block pathways through the polymer [9,10], which impairs the separation process, dedicated studies must be conducted to shed light on the sorption occurrence of the VFAs in each membrane testes here.

3.3.3. pH and conductivity of feed and receiver solutions

Fig. 10 shows the pH vs. time profiles of the feed (Fig. 10 a,b,c) and receiver (Fig. 10 d,e,f) solutions throughout the ED experiments conducted with Ralex, Fumasep and PC200D under each voltage value. The small variations (between 6 and 6.2 for the feed and 5.7 – 6.2 for the receiver) in the initial pH values are due to the recirculation of distilled water through the compartments/reservoirs before the experiments.

As shown in Fig. 10, the feed pH maintained virtually constant over time under low voltages and decreased strongly under high voltages, despite the transfer of the acids (VFAs) to the receiver compartment. This reduction is explained by the occurrence of water dissociation reaction at the diluate side of the AEMs. Note in Fig. 10 that the final pH values of feed solution of the tests conducted with Fumasep and PC200D at 2.74 V, 2.82 V and 2.88 V was lower than 5, while for Ralex it occurred only at 2.88 V. This indicates the formation of protonated VFAs at these voltage conditions and supports the discussions on chronopotentiometry (Section 3.2) and the decrease in MB% for Ralex and Fumasep due to potential VFAs evaporation in their free form. As the pH at the diluate interface of AEMs is considerably lower than in the bulk solution [38,47], the formation of uncharged VFAs at the membrane surface may also have occurred at lower voltage values. The less intense pH reduction of the feed solution with Ralex than with Fumasep and PC200D indicates a less intense water dissociation at the former, which also agrees with the previous discussions. The intense pH reduction of the feed solution to values lower than 5 over time under the highest voltage values (2.74 V – 2.88 V) should be avoided, since the uncharged species formed are not transferred through the membranes and, in this case, a fraction of the energy consumed is wasted. Besides, it was verified (Table 3) that the application of high voltages reduces the fractionation degree of the VFAs.

The pH profile of the receiver solution showed distinct behaviors depending on the membrane under investigation. As shown in Fig. 10d, the receiver pH with Ralex dropped rapidly (0.5 h) and the drop intensity increased considerably with the voltage applied. As Ralex did not show greater transfer of VFAs from the feed solution when compared with the other membranes, this drop could be explained by the desorption of VFAs that were sorbed in Ralex in the previous tests, which supports the unexpected behavior of Ralex on VFAs flux and mass balance discussed in Section 3.3.2. The pH drop intensity increased significantly with increasing cell voltage due to the enhanced driving force that favored the VFAs desorption. The receiver solution pH increased over time due to the transport of OH^- ions present initially in the feed solution, in addition to the OH^- ions possibly generated by water dissociation at the membrane's diluate interface. The pH profiles of the receiver solution with Fumasep (Fig. 10e) and PC200D (Fig. 10f) membranes showed another behavior: under no (0 V) or low voltage values, the pH increased in a short time (0.5 h) and remained constant or decreased over time (1h-7h). The pH increase in a short time can be explained by the preferential transport of OH^- ions initially present in the feed solution due to their much smaller size compared to VFAs, while the constant or decreasing pH behavior can be explained by the transport of VFAs to the receiver solution over time. Under high voltage values, the pH of the receiver solution with Fumasep and PC200D dropped rapidly (0.5 h) and remained practically constant (showing a subtle increase) over time (1h-7h), which can be explained by the intense transfer of VFAs in a short time and the transfer of OH^- ions from the feed solution under intense water dissociation together with electroconvection at longer times. As the presence of VFAs and OH^- in the receiver solution causes opposing effects on its pH, it remained virtually constant over time.

The conductivity profiles of the feed and receiver solutions are shown in Figure S11 (see supplementary material). The membranes exhibited similar behaviors. For the feed solutions, the conductivity slightly increased under no (0 V) and low voltages (1.72 V), while decreased considerably under the other voltages (2.22 V – 2.88 V). The increase observed for 0 V and 1.72 V can be explained by the higher

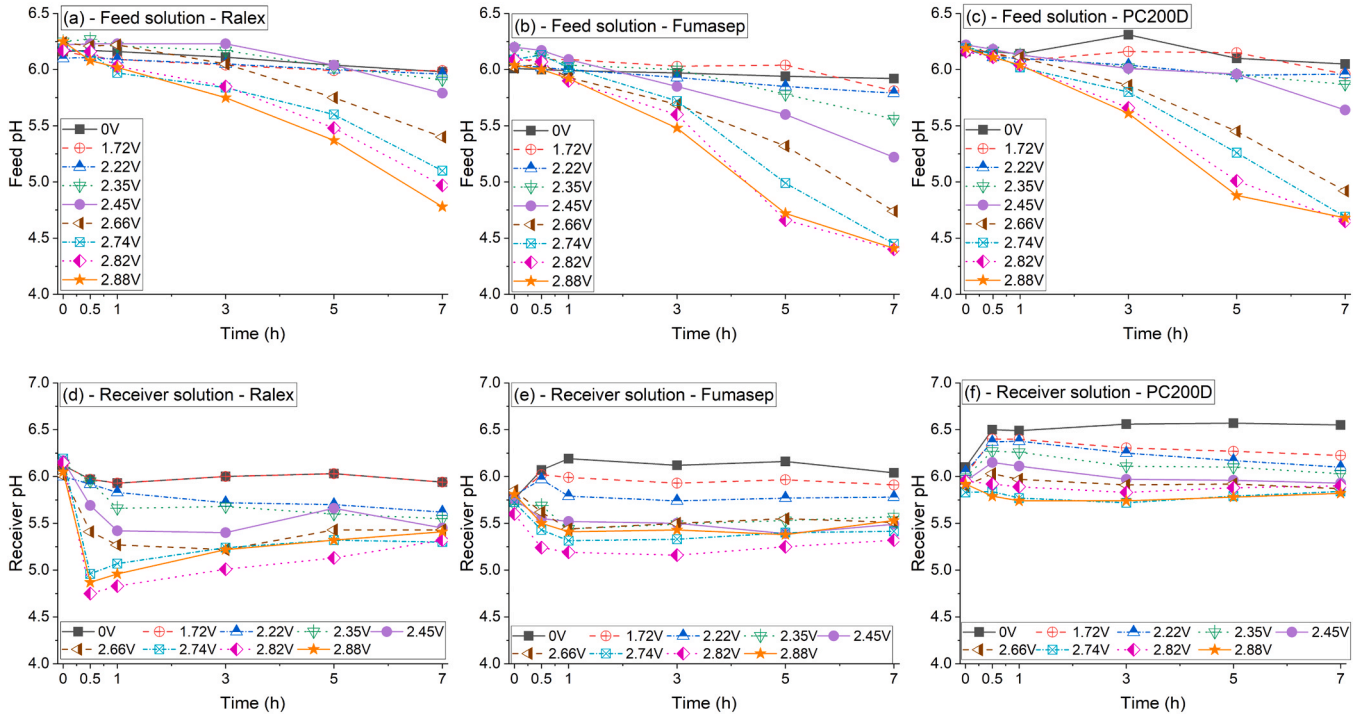

Fig. 10. – Representative pH time profiles of the feed (a,b,c) and receiver (d,e,f) solutions obtained under application of distinct cell voltage values (0 V – 2.88 V) with Ralex, Fumasep and PC200D membranes.

conductivity of the initial receiver solution (~9.5 mS/cm) than the feed solution (~6 mS/cm), favoring the transport of Cl^- ions through the AEM by diffusion. When voltages between 2.22 V – 2.88 V were applied, the conductivity of the feed solutions decreased expectedly because the solution became more diluted. The receiver solutions exhibited the opposite behavior for all membranes: a slight reduction over time in conductivity under no (0 V) and low voltages (1.72 V) due to the transport of Cl^- ions by diffusion to the feed solution and a strong increase under the other voltages (2.22 V – 2.88 V) due to the increase in VFAs concentration throughout the experiments.

3.3.4. *Practical implications of the results in the production of PHAs*

The membrane type, applied voltage, and operating time strongly influence the fractionation degree of VFAs in the production of PHAs. For all membranes tested, it was observed that under high voltages and extended durations, the simultaneous transfer of all VFAs (acetic, propionic, butyric and valeric acids) through the AEMs is intensified, thereby reducing the fractionation degree of the VFAs, which are recovered together in the receiver solution. Conversely, under the application of low to moderate voltages and shorter times, higher degrees of fractionation are achieved. In this scenario, the separation of acetic and propionic acids (transferred to the receiver solution) from butyric and valeric acids (retained in the feed solution) is intensified. However, in this case, lower PE% values for all VFAs are obtained. Therefore, it is necessary to consider a trade-off between the desired PE % values and fractionation degree when selecting the voltage and operating time.

Concerning the membrane characteristics, the type of functional groups (composed of quaternary ammonium and/or tertiary amines) was found to be the factor with the greatest impact on the fractionation degree. Among the membranes evaluated, the use of PC200D is most recommended as it contains tertiary amines, achieving PE% ratios of VFAs pairs significantly higher than those of other membranes, particularly under moderate voltage values. This is related to the ability of tertiary amines to promote the transport of shorter-chain VFAs (acetic and propionic acids) while retaining longer-chain VFAs (butyric and valeric acids). With PC200D, $(PE_{Ac}+PE_{Prop})/(PE_{But}+PE_{Val})$ ratios of 1.4 are obtained under 2.35 V (7 hours), 2.45 V (5 hours), 2.66 V (3 hours), and 2.74 V (3 hours). Although the voltage of 2.74 V allows for a high degree of fractionation, voltages equal to or greater than this value should be avoided because the intense water dissociation on the membrane surface, facilitated by the tertiary amines, leads to a sharp reduction in the solution's pH and the consequent formation of uncharged species, which could result in increased energy consumption not associated with the transfer of VFAs. Therefore, it is suggested that low to moderate voltage values are applied, preferably between 2.35 V and 2.45 V, as these allow for high percent extraction values of acetic and propionic acids (up to 75 % under 2.35 V, and 85 % under 2.45 V) and high $(PE_{Ac}+PE_{Prop})/(PE_{But}+PE_{Val})$ ratios (around 1.5).

If the aim of the electrodialysis operation is to recover all VFAs in the receiver solution rather than fractionating them, the use of Fumasep should be considered, as this membrane showed PE% values for acetic and propionic acids similar to the PC200D, while the PE% of butyric and valeric acids obtained with Fumasep were also high. Considering the application of ED evaluated in this study, it is suggested that the use of the Ralex membrane is avoided, despite being more resistant and affordable, due to the considerably lower PE% values and PE% ratios obtained for all VFAs.

Lastly, it is worth mentioning that the solutions tested herein are synthetic and do not contain other components typically present in real biological process solutions, such as nutrients and other cationic and anionic species [21]. The presence of nutrients in real solutions (usually present as NH_4^+), in addition to Na^+, and other cationic species in trace concentrations should not affect the transfer of VFAs as they are co-ions (present a positive charge), meaning they are repelled by the AEM. The presence of other anionic species (counter-ions) in real solutions, such as Cl^- and other species in trace concentrations, should also not alter the results of VFAs' fractionation degree observed herein, as no species/complexes are formed between the VFAs and Cl^- ions, meaning they are transferred independently through the AEM. However, the presence of Cl^- ions and other anionic species in trace concentrations may alter the time required to achieve the PE% values obtained herein. Therefore, it is suggested that a dedicated study be conducted to evaluate the relationship between voltage and time using the PC200D membrane and a real fermentative process solution.

From a PHA production perspective, separating the VFA mixture—comprising acetic, propionic, butyric, and valeric acids—into two distinct solutions (one enriched with acetic and propionic acids and the other with butyric and valeric acids) offers both economic and efficiency benefits. Studies have demonstrated that PHA-accumulating MMCs generally preferentially consume longer-chain VFAs (butyric and valeric acids) for PHA synthesis before utilizing shorter-chain VFAs (acetic and propionic acids) [48]. This selective consumption behavior impacts both the efficiency and duration of the PHA accumulation stage.

Operators during PHA accumulation face two options regarding pulse-wise feeding: i) introduce a new carbon pulse once butyric and valeric acids are depleted, which can accelerate the accumulation process and potentially increase PHA storage and yields. However, this approach may result in the accumulation of acetic and propionic acids, which could reach high concentrations, potentially inhibiting the culture. Additionally, treatment of the effluent is required before safe disposal; or ii) wait for the culture to consume the less-preferred VFAs after the butyric and valeric acids are depleted. This approach may lead to longer accumulation times and potentially lower maximum PHA storage and yields, as the culture might enter a famine state for butyric and valeric acids. However, the advantage is that it produces a carbon-free effluent, thereby eliminating the need for further treatment.

Fractionating the VFA mixture prior to use in PHA accumulation can address these challenges, enhancing PHA storage in the biomass and improving overall PHA yields. Additionally, optimizing the butyric/valeric ratio during fractionation can enable tailored production of P (3HB-co-HV) copolymers with varying 3HV content, resulting in polymers with diverse properties and a broader range of potential applications.

Moreover, the solution with acetic and propionic acid content (receiver) could be directed towards various bioprocesses. For instance, it could be utilized in biogas production using anaerobic digestion, where acetic acid serves as a primary methane precursor [49]. Alternatively, the solution could be employed in aerobic granular sludge (AGS) reactors for the production of extracellular polymeric substances (EPS), as these systems have been shown to effectively use simple wastewater containing acetate and propionate as carbon sources [50].

4. Conclusions

Systematic electrodialysis experiments were conducted using two homogenous and one heterogenous AEMs and applying distinct cell voltages to evaluate the recovery and fractionation of four VFAs commonly present in fermented solutions used for PHA production. All membranes exhibited a decrease in the fractionation degree of VFAs as the voltage and/or time increased. Conversely, lower PE% values were obtained at lower voltages and shorter durations. Therefore, a trade-off between the desired high fractionation degree and high PE% values must be considered.

Among the evaluated membranes, the PC200D demonstrated the highest capacity for VFAs fractionation, which might be attributed to the presence of tertiary amines in its fixed functional groups. With the PC200D, PE% values of around 80 % were obtained for acetic and propionic acids, achieving a PE% ratio for the pairs of acetic+propionic and butyric+valeric of 1.4 under voltages of up to 2.45 V. Voltages above 2.45 V are not recommended to avoid the occurrence of intense water dissociation at the membrane surface, and a consequent increase

in energy consumption not associated with an enhancement in the VFAs degree of recovery.

The promising results obtained with the PC200D indicate that the proportion of tertiary amines in the membrane functional groups must be further exploited as a potential way for increasing the degree of electrodialytic separation of VFAs. It is therefore suggested that dedicated studies should be conducted to evaluate other commercial anion-exchange membranes containing tertiary amines and/or to develop membranes presenting different proportions of quaternary/tertiary amines in order to further improve their VFAs fractionation properties.

Considering PHA production, our findings support the valorization of solutions rich in butyric and valeric acids (retained in the feed) during the PHA accumulation phase. This approach could enhance PHA storage in the biomass and improve overall PHA yield, leading to increased productivity. Conversely, the solution with higher concentrations of acetic and propionic acids (receiver) could be redirected to alternative bioprocesses, such as biogas production or EPS synthesis.

CRediT authorship contribution statement

Valentín Pérez-Herranz: Writing – review & editing, Supervision, Project administration, Funding acquisition. **Svetlozar Velizarov:** Writing – review & editing, Supervision, Resources, Project administration, Funding acquisition, Conceptualization. **Kayo Santana Barros:** Writing – review & editing, Writing – original draft, Visualization, Validation, Methodology, Investigation, Formal analysis, Data curation, Conceptualization. **Bruno Marreiros:** Writing – review & editing, Conceptualization. **Maria Reis:** Writing – review & editing, Supervision, Resources, Project administration, Funding acquisition. **João Crespo:** Writing – review & editing, Supervision, Resources, Project administration, Funding acquisition.

Declaration of Competing Interest

The authors declare that they have no known competing financial interests or personal relationships that could have appeared to influence the work reported in this paper.

Acknowledgments

Universitat Politècnica de València and Ministerio de Universidades de España (Plan de Recuperación, Transformación y Resiliencia – financed by European Union - Next GenerationEU) are acknowledged for the post-doctoral research grant attributed to Kayo Santana Barros. This work was financed by Fundação para a Ciência e a Tecnologia, I.P., Lisbon, Portugal in the scope of the SaltiPHA (PTDC/BTA-BTA/30902/2017), Laboratório Associado para a Química Verde - Tecnologias e Processos Limpos (UIDB/50006/2020 and UIDP/50006/2020), Research Unit on Applied Molecular Biosciences – UCIBIO (UIDP/04378/2020 and UIDB/04378/2020), Associate Laboratory Institute for Health and Bioeconomy - i4HB (LA/P/0140/2020).

Appendix A. Supporting information

Supplementary data associated with this article can be found in the online version at doi:10.1016/j.jece.2024.114457.

Data Availability

Data will be made available on request.

References

[1] B.C. Marreiros, M. Carvalheira, C. Henriques, D. Pequito, Y. Nguyen, R.G. Solstad, J.J. Eksteen, M.A.M. Reis, Pilot-scale valorisation of salmon peptone into polyhydroxyalkanoates by mixed microbial cultures under conditions of high ammonia concentration, J. Environ. Chem. Eng. 11 (2023) 110100, https://doi.org/10.1016/j.jece.2023.110100.

[2] Polyhydroxyalkanoates market size, (2024). ⟨https://www.statista.com/statistics/1010383/global-polyhydroxyalkanoate-market-size/⟩. (accessed March 29, 2024).

[3] S. Aghapour Aktij, A. Zirehpour, A. Mollahosseini, M.J. Taherzadeh, A. Tiraferri, A. Rahimpour, Feasibility of membrane processes for the recovery and purification of bio-based volatile fatty acids: a comprehensive review, J. Ind. Eng. Chem. 81 (2020) 24–40, https://doi.org/10.1016/j.jiec.2019.09.009.

[4] M. Ramos-Suarez, Y. Zhang, V. Outram, Current perspectives on acidogenic fermentation to produce volatile fatty acids from waste, Rev. Environ. Sci. Bio/Technol. 20 (2021) 439–478, https://doi.org/10.1007/s11157-021-09566-0.

[5] L. Bazinet, T.R. Geoffroy, Electrodialytic processes: market overview, membrane phenomena, recent developments and sustainable strategies, Membr. (Basel) 10 (2020) 221, https://doi.org/10.3390/membranes10090221.

[6] R.J. Jones, J. Massanet-Nicolau, A. Guwy, G.C. Premier, R.M. Dinsdale, M. Reilly, Removal and recovery of inhibitory volatile fatty acids from mixed acid fermentations by conventional electrodialysis, Bioresour. Technol. 189 (2015) 279–284, https://doi.org/10.1016/j.biortech.2015.04.001.

[7] R. Chalmers Brown, R. Tuffou, J. Massanet Nicolau, R. Dinsdale, A. Guwy, Overcoming nutrient loss during volatile fatty acid recovery from fermentation media by addition of electrodialysis to a polytetrafluoroethylene membrane stack, Bioresour. Technol. 301 (2020) 122543, https://doi.org/10.1016/j.biortech.2019.122543.

[8] A. Scoma, F. Varela-Corredor, L. Bertin, C. Gostoli, S. Bandini, Recovery of VFAs from anaerobic digestion of dephenolized Olive Mill Wastewaters by Electrodialysis, Sep. Purif. Technol. 159 (2016) 81–91, https://doi.org/10.1016/j.seppur.2015.12.029.

[9] Q. Wang, G.Q. Chen, S.E. Kentish, Sorption and diffusion of organic acid ions in anion exchange membranes: acetate and lactate ions as a case study, J. Memb. Sci. 614 (2020) 118534, https://doi.org/10.1016/j.memsci.2020.118534.

[10] M.-S. Kang, S.-H. Cho, S.-H. Kim, Y.-J. Choi, S.-H. Moon, Electrodialytic separation characteristics of large molecular organic acid in highly water-swollen cation-exchange membranes, J. Memb. Sci. 222 (2003) 149–161, https://doi.org/10.1016/S0376-7388(03)00267-9.

[11] V.V. Nikonenko, A.V. Kovalenko, M.K. Urtenov, N.D. Pismenskaya, J. Han, P. Sistat, G. Pourcelly, Desalination at overlimiting currents: state-of-the-art and perspectives, Desalination 342 (2014) 85–106, https://doi.org/10.1016/j.desal.2014.01.008.

[12] N. Pismenskaia, P. Sistat, P. Huguet, V. Nikonenko, G. Pourcelly, Chronopotentiometry applied to the study of ion transfer through anion exchange membranes, J. Memb. Sci. 228 (2004) 65–76, https://doi.org/10.1016/j.memsci.2003.09.012.

[13] V.V. Gil, M.A. Andreeva, L. Jansezian, J. Han, N.D. Pismenskaya, V.V. Nikonenko, C. Larchet, L. Dammak, Impact of heterogeneous cation-exchange membrane surface modification on chronopotentiometric and current–voltage characteristics in NaCl, CaCl2 and MgCl2 solutions, Electrochim. Acta 281 (2018) 472–485, https://doi.org/10.1016/j.electacta.2018.05.195.

[14] D. Cardoso, L. Stéphano, M. Antônio, S. Rodrigues, A. Moura, J. Alberto, S. Tenório, Water recovery from acid mine drainage by electrodialysis, Miner. Eng. 40 (2013) 82–89, https://doi.org/10.1016/j.mineng.2012.08.005.

[15] S.D. Bittencourt, L. Marder, T. Benvenuti, J.Z. Ferreira, A.M. Bernardes, Analysis of different current density conditions in the electrodialysis of zinc electroplating process solution, Sep. Sci. Technol. 52 (2017) 2079–2089, https://doi.org/10.1080/01496395.2017.1310896.

[16] P. Altmeier, H. Bolz, G. Schwitzgebel, New anion exchange membranes for the electrodialytic treatment of acids, Pap. Present. Elev. Int. Forum Electro Chem. Ind. (1997).

[17] Website of MEGA a.s.: AMH-PES Data Sheet, (2024). ⟨https://www.mega.cz/files/datasheet/MEGA-RALEX-AMH-PES-en.pdf⟩ (Accessed April 27, 2024).

[18] FuelCellStore, (2022). ⟨https://www.fuelcellstore.com/fuel-cell-components/membranes/cation-exchange-membrane/fumasep-fks-pet-130⟩ (Accessed December 6, 2022).

[19] D. Arslan, Y. Zhang, K.J.J. Steinbusch, L. Diels, H.V.M. Hamelers, C.J.N. Buisman, H. De Wever, In-situ carboxylate recovery and simultaneous pH control with tailor-configured bipolar membrane electrodialysis during continuous mixed culture fermentation, Sep. Purif. Technol. 175 (2017) 27–35, https://doi.org/10.1016/j.seppur.2016.11.032.

[20] M. Pessoa-Lopes, J.G. Crespo, S. Velizarov, Arsenate removal from sulphate-containing water streams by an ion-exchange membrane process, Sep. Purif. Technol. 166 (2016) 125–134, https://doi.org/10.1016/j.seppur.2016.04.032.

[21] K.S. Barros, M. Carvalheira, B.C. Marreiros, M.A.M. Reis, J.G. Crespo, V. Pérez-Herranz, S. Velizarov, Donnan dialysis for recovering ammonium from fermentation solutions rich in volatile fatty acids, Membr. (Basel) 13 (2023) 347, https://doi.org/10.3390/membranes13030347.

[22] Website of MEGA a.s.: CMH-PES Data Sheet, (2024). ⟨https://www.mega.cz/files/datasheet/MEGA-RALEX-CMH-PES-en.pdf⟩ (Accessed April 27, 2024).

[23] R. Liu, Y. Wang, G. Wu, J. Luo, S. Wang, Development of a selective electrodialysis for nutrient recovery and desalination during secondary effluent treatment, Chem. Eng. J. 322 (2017) 224–233, https://doi.org/10.1016/j.cej.2017.03.149.

[24] D.A. Cowan, J.H. Brown, Effect of turbulence on limiting current in electrodialysis cells, Ind. Eng. Chem. 51 (1959) 1445–1448, https://doi.org/10.1021/ie50600a026.

[25] S. Koter, M. Zator, Determination of the electrolyte and osmotic permeability coefficients by conductometric and emf methods, Desalination 162 (2004) 373–381, https://doi.org/10.1016/S0011-9164(04)00071-2.

[26] C. Ponce-De-León, C.T.J. Low, G. Kear, F.C. Walsh, Strategies for the determination of the convective-diffusion limiting current from steady state linear sweep voltammetry, J. Appl. Electrochem. 37 (2007) 1261–1270, https://doi.org/10.1007/s10800-007-9392-3.
[27] E.H. Rotta, C.S. Bitencourt, L. Marder, A.M. Bernardes, Phosphorus recovery from low phosphate-containing solution by electrodialysis, J. Memb. Sci. 573 (2019) 293–300, https://doi.org/10.1016/j.memsci.2018.12.020.
[28] E.D. Belashova, N.A. Melnik, N.D. Pismenskaya, K.A. Shevtsova, A.V. Nebavsky, K. A. Lebedev, V.V. Nikonenko, Overlimiting mass transfer through cation-exchange membranes modified by Nafion film and carbon nanotubes, Electrochim. Acta 59 (2012) 412–423, https://doi.org/10.1016/j.electacta.2011.10.077.
[29] V.V. Nikonenko, N.D. Pismenskaya, E.I. Belova, P. Sistat, P. Huguet, G. Pourcelly, C. Larchet, Intensive current transfer in membrane systems: modelling, mechanisms and application in electrodialysis, Adv. Colloid Interface Sci. 160 (2010) 101–123, https://doi.org/10.1016/j.cis.2010.08.001.
[30] L. Wang, Z. Li, Z. Xu, F. Zhang, J.E. Efome, N. Li, Proton blockage membrane with tertiary amine groups for concentration of sulfonic acid in electrodialysis, J. Memb. Sci. 555 (2018) 78–87, https://doi.org/10.1016/j.memsci.2018.03.011.
[31] Z. Yao, Y. Li, Y. Cui, K. Zheng, B. Zhu, H. Xu, L. Zhu, Tertiary amine block copolymer containing ultrafiltration membrane with pH-dependent macromolecule sieving and Cr(VI) removal properties, Desalination 355 (2015) 91–98, https://doi.org/10.1016/j.desal.2014.10.030.
[32] E. Korzhova, N. Pismenskaya, D. Lopatin, O. Baranov, L. Dammak, V. Nikonenko, Effect of surface hydrophobization on chronopotentiometric behavior of an AMX anion-exchange membrane at overlimiting currents, J. Memb. Sci. 500 (2016) 161–170, https://doi.org/10.1016/j.memsci.2015.11.018.
[33] J.-H. Choi, H.-J. Lee, S.-H. Moon, Effects of electrolytes on the transport phenomena in a cation-exchange membrane, J. Colloid Interface Sci. 238 (2001) 188–195, https://doi.org/10.1006/jcis.2001.7510.
[34] Z. Li, W. Qin, Y. Dai, Liquid-liquid equilibria of acetic, propionic, butyric, and valeric acids with trioctylamine as extractant, J. Chem. Eng. Data. 47 (2002) 843–848, https://doi.org/10.1021/je015526t.
[35] H. Strathmann, Electrodialysis, a mature technology with a multitude of new applications, Desalination 264 (2010) 268–288, https://doi.org/10.1016/j.desal.2010.04.069.
[36] N.D. Pismenskaya, V.V. Nikonenko, E.I. Belova, G.Y. Lopatkova, P. Sistat, G. Pourcelly, K. Larshe, Coupled convection of solution near the surface of ion-exchange membranes in intensive current regimes, Russ. J. Electrochem. 43 (2007) 307–327, https://doi.org/10.1134/S102319350703010X.
[37] E.I. Belova, G.Y. Lopatkova, N.D. Pismenskaya, V.V. Nikonenko, C. Larchet, G. Pourcelly, Effect of anion-exchange membrane surface properties on mechanisms of overlimiting mass transfer, J. Phys. Chem. B. 110 (2006) 13458–13469, https://doi.org/10.1021/jp062433f.
[38] N.D. Pismenskaya, O.A. Rybalkina, A.E. Kozmai, K.A. Tsygurina, E.D. Melnikova, V.V. Nikonenko, Generation of H+ and OH− ions in anion-exchange membrane/ampholyte-containing solution systems: a study using electrochemical impedance spectroscopy, J. Memb. Sci. 601 (2020) 117920, https://doi.org/10.1016/j.memsci.2020.117920.
[39] P. Długołecki, B. Anet, S.J. Metz, K. Nijmeijer, M. Wessling, Transport limitations in ion exchange membranes at low salt concentrations, J. Memb. Sci. 346 (2010) 163–171, https://doi.org/10.1016/j.memsci.2009.09.033.
[40] R.K. Nagarale, G.S. Gohil, V.K. Shahi, Recent developments on ion-exchange membranes and electro-membrane processes, Adv. Colloid Interface Sci. 119 (2006) 97–130, https://doi.org/10.1016/j.cis.2005.09.005.
[41] D.R. Lide, Handbook of Chemistry and Physics, CRC Press, New York, 1997.
[42] C.L. Yaws, Diffusion Coefficient in Water – Organic Compounds. Transp. Prop. Chem. Hydrocarb., Elsevier, 2009, pp. 502–593, https://doi.org/10.1016/B978-0-8155-2039-9.50017-X.
[43] B. Tao, P. Passanha, P. Kumi, V. Wilson, D. Jones, S. Esteves, Recovery and concentration of thermally hydrolysed waste activated sludge derived volatile fatty acids and nutrients by microfiltration, electrodialysis and struvite precipitation for polyhydroxyalkanoates production, Chem. Eng. J. 295 (2016) 11–19, https://doi.org/10.1016/j.cej.2016.03.036.
[44] T. Rottiers, K. Ghyselbrecht, B. Meesschaert, B. Van der Bruggen, L. Pinoy, Influence of the type of anion membrane on solvent flux and back diffusion in electrodialysis of concentrated NaCl solutions, Chem. Eng. Sci. 113 (2014) 95–100, https://doi.org/10.1016/j.ces.2014.04.008.
[45] R. Epsztein, E. Shaulsky, M. Qin, M. Elimelech, Activation behavior for ion permeation in ion-exchange membranes: role of ion dehydration in selective transport, J. Memb. Sci. 580 (2019) 316–326, https://doi.org/10.1016/j.memsci.2019.02.009.
[46] M.A. Izquierdo-Gil, V.M. Barragán, J.P.G. Villaluenga, M.P. Godino, Water uptake and salt transport through Nafion cation-exchange membranes with different thicknesses, Chem. Eng. Sci. 72 (2012) 1–9, https://doi.org/10.1016/j.ces.2011.12.040.
[47] O.A. Rybalkina, M.V. Sharafan, V.V. Nikonenko, N.D. Pismenskaya, Two mechanisms of H+/OH− ion generation in anion-exchange membrane systems with polybasic acid salt solutions, J. Memb. Sci. 651 (2022) 120449, https://doi.org/10.1016/j.memsci.2022.120449.
[48] J.M. Carvalho, B.C. Marreiros, M.A.M. Reis, Polyhydroxyalkanoates production by mixed microbial culture under high salinity, Sustain 14 (2022) 1–15, https://doi.org/10.3390/su14031346.
[49] T. Fenchel, G.M. King, T.H. Blackburn, Bacterial Metabolism. Bact. Biogeochem., Elsevier, 2012, pp. 1–34, https://doi.org/10.1016/B978-0-12-415836-8.00001-3.
[50] A. Adler, C. Holliger, Multistability and reversibility of aerobic granular sludge microbial communities upon changes from simple to complex synthetic wastewater and back, Front. Microbiol. 11 (2020) 1–20, https://doi.org/10.3389/fmicb.2020.574361.